MINISTRY OF SUPPLY

AERONAUTICAL RESEARCH COUNCIL
REPORTS AND MEMORANDA

Force and Moment Measurements on a Conical Body and a Rectangular Wing, Separately and in Combination, at Mach Number 1·94

By

J. R. ANDERSON, B.Sc.(Eng.), D.I.C., and D. TREADGOLD, D.C.Ae.

LONDON: HER MAJESTY'S STATIONERY OFFICE

1956

SEVEN SHILLINGS NET

Force and Moment Measurements on a Conical Body and a Rectangular Wing, Separately and in Combination, at Mach Number 1·94

By

J. R. Anderson, B.Sc. (Eng.), D.I.C. and D. Treadgold, D.C.Ae.

Communicated by the Principal Director of Scientific Research (Air),
Ministry of Supply

Reports and Memoranda No. 2864[*]

August, 1951

Summary.—Results are given of wind-tunnel measurements at $M = 1·94$ of lift, drag and pitching moment at small angles of incidence on two cones, three rectangular wings and on the six derived cone-wing combinations. A description of the tests and a comparison with theory are also included.

The agreement between theory and experiment for the lift of the isolated cones and wings is good; however, for the drag and centre of pressure, agreement is a little less satisfactory. The measured lift of the cone-wing combinations exceeded that estimated, whereas the measured centre-of-pressure position agreed remarkably well with the estimated position. Agreement between measurement and theory for the lowest aspect ratio wing was improved when a correction was applied for the influence on the cone of the downwash generated by the wings.

An unsuccessful attempt was made to measure the forces and moments on each component of the cone-wing combination independently, whilst under the influence of the flow field of the other.

---

1. *Introduction.*—This report describes lift, drag and pitching-moment measurements on a series of wing-body combinations, the wings being rectangular of aspect ratios 3, 4 and 6, the bodies right circular cones of nominal total vertex angles 10 and 15 deg. The measurements include those made on isolated bodies and wings. The tests were intended to be carried out over a range of Mach numbers, but insufficient tunnel time limited the work to $M = 1·94$. At this speed, the Reynolds number of the tests was about 0·36 million per inch, or 0·27 million based on wing chord.

The main object of the tests was to compare the measured lifts and centres of pressure of the combinations with those given by theory, including the effect of wing-body mutual interference. An attempt to measure the interference effects on the individual components in the combination by employing a dummy supporting sting technique failed. The forces and moments acting on the isolated bodies and wings were required to check the accuracy of the simple assumptions of the wing-body interference theory, and also to compare with higher order theoretical estimates.

The measurements were made in the No. 8 (10-in. × 9-in.) Supersonic Wind Tunnel during the period November 1949 to March 1950, using a three-component mechanical-type balance, both of which are described briefly in section 3. Section 2 contains details of design and manufacture of the wings and bodies, while section 4 describes the force and moment measurements made. These are discussed in detail in section 5 and compared with theoretical calculations, the general conclusions which arise from the investigation being summarized in section 6. A brief résumé of the interference theory employed is contained in an Appendix at the end of the Report.

---

2. *Model Design.*—The maximum size of the model was governed by that of the tunnel and the minimum Mach number at which the model was expected to be tested. Measurements over the Mach number range 1·5 to 2·4 were originally intended, and the maximum length of model was therefore determined by the condition that at $M = 1·5$ the shock from the nose when reflected from the edge of the supersonic jet should pass behind the model. The theoretical maximum allowable blockage at this Mach number was about 9 per cent, but since the effect of two struts behind the model was unknown, a base diameter of 1·5 in. was assumed, corresponding to about 3 per cent blockage at zero incidence.

The shape of the model, conical body with rectangular wings, was chosen to enable direct checks against the theory of Kirkby and Robinson[1] (1947) to be obtained. Two cones, nominally of 10 and 15-deg total angle, were manufactured to obtain the advantages both of conical flow and also of relatively slim bodies. The measured cone angles were 9·8 and 15·7 deg respectively. The rectangular wings were of symmetrical double-wedge section, 10 per cent maximum thickness/chord ratio, and were of aspect ratios 3, 4 and 6. The wing chord was 0·75 in. Fig. 1 shows a photograph of cones and wings.

The balance of the No. 8 Supersonic Wind Tunnel is provided with a second, 'dummy', model support, which enables tare forces on the model supporting sting (balance sting) to be measured under the correct conditions, the model being supported on the dummy sting. This arrangement was to be used in these tests to enable either wing or body to be mounted on the balance sting and the other on the dummy sting, allowing the forces on the one component to be measured independently of the other under flow conditions corresponding to the complete model configuration. It was thus hoped that interference effects on wings and bodies could be obtained separately. To take advantage of this arrangement, the wing and body were designed to be fitted to the stings independently, the gap in the body being made large enough to allow a small clearance all round the wing. The mechanism of this arrangement is illustrated in Fig. 2.

Fig. 3 shows sketches of cones and wings with the Mach angles from cone tips and wing tips (for $M = 1·94$) drawn in to illustrate the proportions of the assembled models. It is seen that the wings lie inside the Mach cone from the body apex except in one case, and that part of the body lies inside the Mach cone from the wing tip for wings of aspect ratios 3 and 4.

At the Mach number of the tests described, $M = 1·94$, the Reynolds number achieved in the tunnel was about $0·36 \times 10^6$ per inch. The Reynolds number for the wings was thus about $0·27 \times 10^6$ based on chord length, and for 10 and 15 deg cones, about $3·1 \times 10^6$ and $2·1 \times 10^6$ respectively, based on cone length.

3. *Description of Tunnel and Balance.*—The No. 8 Supersonic Wind Tunnel (Fig. 4) is a continuous-running open-jet tunnel of approximately 10-in. × 9-in. working-section. Air is drawn from the atmosphere through silica gel adsorption drying beds which deliver it to the tunnel at an absolute humidity of about 0·001. The stagnation pressure in the tunnel is thus slightly less than atmospheric. Anderson and Herbert[2] (1951) have shown that the velocity variation over the working-section of the Mach number 1·94 nozzle is not greater than $\pm 0·015$ in Mach number, that is, within about ± 1 per cent. The balance with which the tunnel is equipped is mechanical in operation, measuring moments about each of three separate lateral axes in turn, in terms of the deflection of a calibrated spring required to return the balance to its null deflection position against the aerodynamic loading of the model. Fig. 5 shows two views of the balance, and illustrates the 'dummy' sting arrangement employed for the present tests. The upper sting and strut are dummy in both photographs, the welded support moving in step with the incidence change of the 'live' model by means of synchronised gearing. A brief description of the tunnel and balance has been given elsewhere by one of the present authors[3] (1950).

Previous tests with the balance in this tunnel had shown that considerable shielding of the balance was essential to prevent air currents in the balance chamber, induced by the free jet, from impinging on the live balance members, causing large tare moments of varying magnitude. For this set of tests, it was decided, therefore, to enclose the free jet inside an inner duct, leaving

a clearance round the strut carrying the model as the only means of communication from inside the duct to the outside. This arrangement can be seen in Fig. 6b, which shows the balance chamber with side door removed. The duct was designed to be approximately 2 in. deeper and 1 in. wider than the jet from the supersonic nozzle. Preliminary tests with this arrangement indicated that insufficient precision in measurement of moments was due to the large tare moments arising from the unshielded model sting and strut. The magnitude of these was considerably decreased, resulting in a considerable gain in accuracy, by the temporary shielding illustrated in Fig. 6c, which shows a close-up view of the inside of the duct, the near side plate being removed. All the measurements described here were made with this shielding.

4. *Force and Moment Measurements.*—4.1. *Procedure.*—With the model in position on the live sting, the tunnel was run, and measurements of the deflexion of the calibrated spring needed to return the model to its null (wind off) position were made over a range of small incidences up to 3 deg, each of the three reference axes of the balance being employed in turn. At intervals, readings of barometer, stagnation pressure and temperature upstream of the throat of the nozzle, and pressure at four stations at the base of the model, were made. Then from a knowledge of the spring strength, obtained by previous calibration, the measured deflexions were converted to moments about their respective axes. These were then divided by the free-stream dynamic pressure q (obtained from the stagnation pressure and the Mach number) in order to remove the effect of slight variations in stagnation pressure from one run to another.

This measurement procedure was repeated with the model supported on the dummy sting, yielding values of the tare moments, which were then subtracted from the previous results to give the moments arising from the model alone. These resulting moments were then combined for each value of incidence to yield lift, drag and pitching-moment coefficients. The routine method of reduction is described in Ref. 3.

4.2. *Measurements on Cone Models.*—Measurements were made on both cones and on all combinations of wings and cones. In each case, the clearance gaps in the side of the cone and holes for screwheads, etc., were sealed off and faired into the cone surface with wax. For ease of reference the cones were designated by their total vertex angle, and the wings by their aspect ratios, for example, C10W6 refers to the cone-wing combination consisting of the 10-deg cone and the aspect ratio 6 wing. The results are plotted in Figs. 7 to 10 for 10-deg cone combinations, and Figs. 11 to 14 for the 15-deg cone combinations, in terms of L/q, D/q and M_A/q, that is, lift, drag and moment, divided by free-stream dynamic pressure.

In each case results were corrected to a base pressure equal to the free-stream pressure, using the mean of the measured base pressures so that effectively the base drag is subtracted from the total measured drag. No account was taken here of variation of pressure over the base of the cone, or any effects of incidence on this pressure. The moments plotted are those measured about an axis 1·63 in. behind the wing leading-edge position, that is, an axis 0·85 in. in front ·of the base of the cone.

4.3. *Measurements on Isolated Wings.*—The support systems used for testing the isolated wings were the same as before, the only difference in procedure being in the measurement of tare forces. This measurement included the forces acting on the slim supporting body seen in Fig. 1, the lift on the wings themselves being obtained by difference in the usual manner, as was the centre of pressure. Wing-body interference theory suggested that the measured lifts thus obtained could be expected to be but little different from the lift of the gross wing, due to the carry-over on to the slender body, whereas the centre of pressure would be expected to be very slightly more rearward than the true gross wing value, for the same reason. At the same time, however, it was realised that the broad attachment of the supporting body would be affected by the downwash field from the wing-tip Mach cones to some extent in the combination measurement, but not in the tare measurement. This would probably reduce the measured wing lift and cause

an apparently too far forward centre of pressure to be obtained. The uncertainty of the measurements was thus fairly large.

The differenced results for the wings alone are plotted against incidence in Fig. 15 to 17, again in terms of L/q, D/q, and M_A/q.

4.4. *Attempted Measurement of Interference Components.*—An attempt was made to measure the separate interference effects between cones and wings, that is, the interference on the cone due to the wing and that on the wing due to the cone. The failure to do this lay in the technique adopted, that of mounting one component on to the balance sting and the other on to the dummy sting. This necessitated a clearance between the two components, including a gap round the wing where it entered the cone, which, in effect, falsified the pressure distribution both on cone and on wing, since the upper surface of the wing and the lower both communicated with the interior of the cone. In addition, since the sting to which the wing was attached was led directly out through the base of the cone, both surfaces at the wing root were in communication with the base of the cone, a region of lower pressure, by means of the hollow interior (*see* Fig. 2). Thus an internal flow was possible through the model, from wing root to cone base. The result of this is clearly seen in Fig. 18, which shows lift curves for (1) cone and wing measured together with gap sealed, (2) cone and wing together with gap unsealed, and (3) the sum of the lifts of the wing in the presence of the body and the body in the presence of the wing, the results shown being for the 10-deg cone and wing of aspect ratio 4.

4.5. *Accuracy of Measurement.*—The main errors arise from the setting of model incidence, the mean deviation of the calibration of the balance restoring spring and the accuracy with which the balance is restored to its null position. The errors in setting model incidence arise firstly from the fact that the position of zero incidence as indicated by the balance, $\theta = 0$, did not coincide with the tunnel wind direction, and secondly from the fact that the incidence scale itself was liable to error. The angle between $\theta = 0$ and the wind direction was not measured, but it is in evidence in the lift and moment curves, which do not pass through the origin. The angle varies, due to change in position of the supersonic nozzle from test to test, but in only one case is it greater than $0\cdot25$ deg. It has negligible effect on the determination of lift-curve slope and centre of pressure, and has been ignored. The incidence scale on the balance has been calibrated and found to be consistent to $\pm 0\cdot1$ deg. The calibration of the restoring spring indicates a possible error of the order of ± 1 per cent in lift and measured drag and ± 2 per cent of wing chord in centre of pressure measurement. The sensitivity of the balance and the accuracy of null deflection determination is seen from the plotted curves to be good. The mean deviation of individual lift results from the mean straight line drawn through them between $\pm 1\frac{1}{2}$ deg incidence is of the order of ± 1 per cent of maximum lift measured, a figure which corresponds to about $\pm 0\cdot03$ deg in incidence, which is less than the uncertainty expected in incidence setting.

The accuracy of drag measurement is not great, due to the fact that a large correction has to be made for the base pressure acting on the cone when correcting drag readings to free-stream static pressure conditions. The pressures at four stations round the base of the cone were measured with a view to obtaining as accurate a correction as possible, but these were found to vary from one to another and to show a slight and apparently random variation with incidence. Without making a far more detailed examination of the pressure distribution over the base of the cone, it was considered that using the mean of the measured pressures when correcting the drag, would result in an error of not more than about ± 10 per cent, and that this, in view of the lesser emphasis on drag measurement, was reasonably satisfactory.

5. *Discussion of Results and Comparison with Theory.*—5.1. *Conical Bodies.*—5.1.1. *Lift-curve Slope* (*Fig.* 19).—The measured values of lift-curve slope at zero incidence lie decidedly below both the slender body theory (*see*, for example, Lighthill[4] (1945)), which gives a value 2 when based on body base area, Tsien's theory[6] (1938), and the small-yaw theory of Stone[5] (1948).

4

The two last-mentioned theories indicate a decreasing slope with increasing cone angle, with which the measured values are in agreement, the measurements being about 3 per cent below the values given by Tsien's theory.

5.1.2. *Centre of pressure position (Fig. 19).*—The linearised theory gives the position of the centre of pressure of a cone at 2/3 of its length from the tip. The wind-tunnel measurements show a progressive rearward shift as cone angle is increased, in very good agreement with the small-yaw theory, the discrepancy being less than $\frac{1}{2}$ per cent of body length.

5.1.3. *Drag at zero incidence (Fig. 20).*—The experimental points, corrected for base pressure, are compared with the Taylor-Maccoll head drag coefficient as tabulated by M.I.T.[7] (1947), plus skin friction (C_f) estimates of 0·003, 0·004 and 0·005 based on wetted area. The highest value of C_f tends to agree with the 10-deg cone result, the lowest with the 15-deg cone. This difference is of the order and in the direction expected due to the variation in Reynolds number between the two cases, but the absolute values of C_f are about twice those which might be expected under these test conditions, namely C_f of the order of 0·0025. The discrepancy is most likely due to the lack of accuracy of drag measurement which has been discussed in section 4.5.

5.1.4. *Summary.*—Reasonably good agreement exists between the experimental results and the more accurate small-yaw theory, with respect to lift curve slope and position of centre of pressure. As is to be expected slender body theory becomes increasingly inaccurate as the cone angle increases, the difference from measurement being of the order of + 10 per cent in lift-curve slope and − 1$\frac{1}{2}$ per cent of body length in centre-of-pressure position for the cone of 15-deg total angle. The measurements of drag indicate higher values of skin-friction coefficient than were to be expected but are of doubtful accuracy.

5.2. *Isolated Wings.*—5.2.1. *Lift-curve slope (Fig. 21).*—The experimental results lie consistently below those given by the approximate second-order theory of Bonney[8] (1947), but follow the shape of this curve closely. The discrepancy is of the order of 5 per cent in all cases. The shock-expansion (two-dimensional) value lies between 10 per cent and 15 per cent higher than the measured ones according to aspect ratio.

5.2.2. *Centre of pressure position (Fig. 21).*—The centre-of-pressure position measured for the aspect ratio 6 wing agrees well with the approximate second-order theory, but this agreement may be fortuitous, since the results for the other two aspect ratios show centre of pressures appreciably behind the theoretical estimate.

5.2.3. *Drag at zero incidence (Fig. 21).*—The measured drag coefficients are much less than had been expected. The estimated values are based on the wave drag obtained from the approximate second-order theory together with skin-friction coefficients for both laminar and turbulent boundary layers as given by Cope[9] (1943) for a flat plate.

5.2.4. *Summary of wing results.*—The agreement between theory and experiment as regards lift-curve slope is seen to be good. Comparisons of the measured centres of pressure and minimum drag coefficient with the theoretical estimates show greater discrepancies but are as good as can reasonably be expected of these tests.

5.3. *Wing-Body Combinations.*—The wing-body interference theory with which the experimental results are compared is based on the simple linear theory, with interference effects of the wing on the body obtained from Ferrari[10] (1948) and the effects of the body on the wing obtained from Kirkby and Robinson. A résumé of these theories is contained in the Appendix. A simple correction for the effects of downwash behind the wing, as suggested by Spreiter[14] (1949), is included.

5.3.1. *Lift-curve slope (Fig. 22).*—Experimental values are seen to be somewhat higher than those calculated from interference theory with the exception of the aspect ratio 3 result. The downwash correction, however, brings this result into line with the other two. In actual fact, downwash will affect all wings but that with the highest aspect ratio, as may be seen from Fig. 3.

However, the simple correction has been applied only where the wing-tip Mach cone intersects the body centre-line. Were a complete correction for downwash possible, the corrected results for both aspect ratio 3 and 4 wings would lie slightly higher above the theoretical curve than the present points. The simple gross wing plus slender body result, which has been used extensively as an interference estimate, is also shown, and is seen to give values appreciably lower than experiment.

The fact that the interference theory is based on the linear theory, which has been seen to provide high values for the components, shows that the actual interference effects obtained are higher than those given by the interference theory. This is as might be expected, since there is some experimental evidence which might be taken to show that the upwash field round a body is more intense than theory suggests (*see* Ferrari[11] (1949)).

5.3.2. *Centres of pressure* (*Fig.* 22).—Agreement between measurements and interference theory is seen to be extremely good, with the simple downwash correction applied. The degree to which this correction brings the lower aspect-ratio measurement into line with the others is quite remarkable. The gross wing plus slender body estimate is seen, however, to give a very poor result, giving values about $\frac{1}{4}$-chord length farther forward than the measurements.

5.3.3. *Drag at zero incidence* (*Fig.* 22).—The theoretical estimates shown are based on the approximate second-order theory with laminar skin friction for the net wing, and the theoretical wave drag and a skin-friction coefficient of 0·0025 for both cones. The measured values are in all cases smaller than the estimates, although these have assumed a smaller, more reasonable value of skin-friction coefficient for the cones than the previous cone-alone measurements indicate. The measured variation of drag with aspect ratio is similar to that of the estimate.

6. *Conclusions.*—6.1. Lift-curve slope and centre-of-pressure measurements at zero incidence made on two cones of 10 and 15-deg total angle agree well with cone theory, but do not show particularly good agreement with the slender body theory, becoming worse for increasing cone angle. Measurements of minimum drag show poor agreement with theoretical estimates, but the uncertainty in measurement is of fairly high order.

6.2. Measurements on isolated wings have been found to give fairly good agreement with the theory, with the possible exception of minimum drag.

6.3. Using the particular arrangement of the test apparatus, it was found impossible to measure the forces on one component of the wing-cone configuration independent of the other. This was due firstly to the presence of a clearance gap round the wing root, and secondly to the connection of this gap with the base of the cone, causing a flow from wing root to cone base.

6.4. Measurements of lift-curve slope and centre of pressure at zero incidence on cone-wing combinations agree fairly well with the calculations made on the interference theory. This theory was a combination of Kirkby and Robinson's solution for the interference on the wing and Ferrari's solution for the interference on the body, with a correction applied to allow for the effect of the wing downwash on the rear of the body.

Measurements of drag of the combinations do not agree well with estimates, but show the same trend with increasing wing aspect ratio.

The interference effects calculated from the composite theory lead to closer agreement with measurement, particularly with respect to centre-of-pressure position, than the gross wing plus body approximation, but require more exhaustive computation.

6.5. Before any general conclusions of a firm nature can be drawn, with regard to the accuracy of calculation of body-wing interference, much more precise and exhaustive tests must be made than are described here. It is to be hoped also, that the theory itself is capable of some simplification and improvement.

6.6. No further work along the lines described here is contemplated mainly due to the failure to measure forces on components separately.

LIST OF SYMBOLS

A	Aspect ratio (gross span/chord)
D	Drag
L	Lift
ΔL_B	Interference lift on the body due to presence of the wing
ΔL_W	,, ,, ,, ,, wing ,, ,, ,, ,, ,, body
M	Free-stream Mach number
M_A	Pitching moment referred to main balance axis (1·63 in. behind the wing leading edge, $i.e.$, 0·85 in. in front of base of cone)
ΔM_B	Interference pitching moment on the body due to the presence of the wing (about the wing leading edge)
ΔM_W	Interference pitching moment on the wing due to the presence of the body (about the wing leading edge)
$q = \frac{1}{2}\rho V^2$.	Free-stream dynamic pressure
R	Reynolds number
R_0	Radius of cross-section of the cone at the wing leading-edge station
V	Free-stream velocity
x	Distance measured in the direction of the cone axis with origin at cone apex
α	Model incidence in radians
θ	Balance incidence in degrees
ρ	Free-stream density

REFERENCES

No.	Author	Title, etc.
1	S. Kirby and A. Robinson	Wing body interference at supersonic speeds. R. & M. 2500. April, 1947.
2	J. R. Anderson and P. J. Herbert	The calibration of supersonic nozzles for the No. 8, 10-in. × 9-in. Supersonic Wind Tunnel. Part I: Original Gottingen nozzles and modified nozzles for Mach numbers 1·85 and 2·50. R.A.E. Tech. Note Aero. 2108. A.R.C. 14,267. June, 1951. (Unpublished.)
3	J. R. Anderson	A brief description of the No. 8 (10-in. × 9-in.) Supersonic Wind Tunnel and equipment. R.A.E. Tech. Note Aero. 2072. A.R.C. 13,847. October, 1950. (Unpublished.)
4	M. J. Lighthill	Supersonic flow past bodies of revolution. R. &. M 2003. January, 1945.
5	A. H. Stone	On supersonic flow past a slightly yawing cone. *J. Math. Phys. MIT.* Vol. XXVII, No. 1, pp. 67 to 81. April, 1848
6	H. S. Tsien	Supersonic flow over an inclined body of revolution. *J. Ae. Sci.* Vol. 5, No. 12. October, 1938.
7	Staff of the Computing Section, Centre of Analysis (under direction of Zdenêk Kopal)	Supersonic flow of air around cones. Massachusetts Institute of Technology, Department of Electrical Engineering. Tech. Report No. 3. 1947.
8	A. E. Bonney	Aerodynamic characteristics of rectangular wings at supersonic speeds. *J. Ae. Sci.* Vol. 14, No. 2. February, 1947.
9	W. F. Cope	The turbulent boundary layer in compressible flow. R. & M. 2840. November, 1943.
10	C. Ferrari	Interference between wing and body at supersonic speeds. Theory and numerical applications. *J. Ae. Sci.* Vol. 15, No. 6. January, 1948.
11	C. Ferrari	Interference between wing and body at supersonic speeds—Note on wind-tunnel results and addendum to calculations. *J. Ae. Sci.* Vol.16, No. 9. September, 1949.
12	R. E. Bolz	Note on interference between wing and body at supersonic speeds. *J. Ae. Sci.* Vol. 17, No. 7. July, 1950.
13	P. A. Lagerstrom and M. E. Graham	Downwash and sidewash induced by three-dimensional lifting wings in supersonic flow. Douglas Aircraft Report No. SM-13007. 1947.
14	J. R. Spreiter	Aerodynamic properties of slender wing body combinations at subsonic, transonic and supersonic speeds. N.A.C.A. Tech. Note 1662. July, 1948.

APPENDIX

Theoretical Estimates of Wing-Body Interference on Lift and Centre of Pressure

1. *Introduction.*—In this appendix a brief description is given of the methods used in estimating the effects of wing-body interaction for the rectangular wing and conical body combination of this test.

Broadly, this interaction may be separated into two parts:

(*a*) The interference of the body on the wing

(*b*) The interference of the wing on the body,

where (*a*) includes the influence of the upwash field around the body as well as the modification to the flow field within the Mach cone from the wing leading edge and body junction, whereas (*b*) includes the influence of the wing pressure field on the flow over the adjacent portion of the body, together with the influence of the downwash field behind the wing.

The problem of wing-body interference is therefore seen to be an extremely complex one, and up to the present no satisfactory method exists for its exact solution. Ferrari in Ref. 10 suggests a first stage in an iteration method of solution*, which is basically the method employed in making these present estimates. In addition, however, a crude correction has been included to allow for the influence of the downwash arising from the wing tips.

2. *Method Adopted.*—2.1. *General.*—For convenience the description of the iteration process contained in Ref. 11 is restated here. The method, which is based on the linearised theory, consists of satisfying in turn the boundary conditions on the wing and the body, by means of doublet distributions along the body centre-line and over the surface of the wing, including that portion enclosed by the body. The two sets of boundary conditions to be satisfied are:

$$V_{n1} + V_{n2} + V_{n\infty} = 0 \text{ and } V_{n1}' + V_{n2}' + V_{n\infty}' = 0$$
$$\text{(on the wing)} \qquad\qquad \text{(on the body)}$$

where V_n represents the velocity component normal to the wing
V_n' ,,   ,,   ,,   ,,   ,,   ,,   ,, body

and the suffix 1 denotes the component due to the distribution of doublets Σ_1 over the wing
2 denotes the component due to the distribution Σ_2 along the body centre-line
and ∞ denotes the free-stream component.

The determination of Σ_1 and Σ_2 can be resolved into a system of integral equations of the Volterra type which may be solved by the method of iteration described below.

2.2. *Zero Approximation.*—Step (1). Calculate Σ_1 using the condition $V_{n1} + V_{n\infty} = 0$ where V_{n2} has been taken as zero, *i.e.*, the solution for the isolated wing.

Step (2). Calculate Σ_2 using $V_{n2}' + V_{n\infty}' = 0$ where V_{n2}' has been taken as zero, *i.e.*, the solution for the isolated body.

2.3. *1st Approximation.*—Step (3). Recalculate Σ_2 using $V_{n1}' + V_{n2}' + V_{n\infty}' = 0$ using Σ_1 of step (1) in calculating V_{n1}'.

Step (4). Recalculate Σ_1 using $V_{n1} + V_{n2} + V_{n\infty} = 0$ using Σ_2 of step (2) in calculating V_{n2}.

Further steps in the iteration can easily be formulated; however the amount of labour involved in their solution is prohibitive.

2.4. *Solutions of Steps* (1) *and* (2).—The solution for the isolated wing may be found in Ref. 8, and the nature of the downwash field can be found in Ref. 13. The solution for an isolated cone can be found in Ref. 6 based on the linearised theory and a more exact solution for a slightly yawed cone is to be found in Ref. 5.

---

* It should be noted that corrections to this paper are given by Ferrari himself[11] (1949) and by Bolz[12] (1950).

2.5. *Solution of Step* (3).—This step consists of determining a longitudinal and a normal component of interference lift and moment. The former is the component arising from Σ_1 of step (1) and corresponds to the carrying over of the wing pressure field within the Mach wedges from the leading and trailing edges of the wing. The normal component arises from the addition to the doublet strength Σ_2 of step (1) necessary to ensure the correct boundary condition on the body, which is violated by Σ_1 of step (1). The magnitude and nature of these two components can be seen from Figs. 23 and 24 for the 15-deg cone at Mach numbers of 1·5 and 2·4. The resultant lifts and moments are shown in Fig. 25.

2.6. *Solution of Step* (4).—This step requires the calculation of the upwash around the cone arising from Σ_2 of step (2) which violates the boundary condition on the wing, and then the determination of the additional doublet distribution over the wing necessary to ensure the correct boundary condition on the wing including that portion within the body. This additional doublet distribution has therefore to produce a downwash outside the body equal and opposite to that of Σ_2 of the first step and an upwash over the portion of the wing included in the body. Ferrari's analysis requires the fitting of a trigonometrical polynomial to the discontinuous downwash distribution which results; even taking 32 terms it is not possible to obtain a solution which is not over-sensitive to the fitted points. However for the simple case of an inverse-square variation of upwash outside the body and the above boundary condition inside the body, the problem is readily solved exactly by means of a source distribution method. Results obtained suggest that little error is, in fact, involved in using a simple strip theory as is done by Kirkby and Robinson. Results obtained in this manner are shown in Fig. 26.

2.7. *Downwash Correction.*—A crude estimate is made of the influence on the body of the downwash behind the wing, using the result given by Spreiter[14]. The downwash is assumed to be that on the x-axis behind an isolated rectangular wing given in Ref. 13. The magnitude of this effect in the case of the lowest aspect ratio wing, which is the only one affected under these assumptions, is seen in Fig. 22.

TABLE 1

Experimental Results for Cone Alone at Zero Incidence

Cone angle	10 deg	15 deg
Lift-curve slope $\frac{\partial(L/q)}{\partial\alpha}$	3·28	3·15
Drag D/q	0·187	0·153
C.P. per cent wing chord aft of wing leading-edge position	−51	100

TABLE 2

Experimental Results for the Wings Alone at Zero Incidence

Wing aspect ratio	3	4	6
Lift-curve slope $\frac{\partial(L/q)}{\partial\alpha}$	3·56	4·90	7·49
Drag D/q	0·034	0·054	0·090
C.P. per cent wing chord aft of wing leading edge	53	48	43

9

TABLE 3

Experimental Results for the Cone-Wing Combinations at Zero Incidence

	Wing aspect ratio	3	4	6
10-deg Cone	Lift-curve slope $\frac{\partial(L/q)}{\partial\alpha}$	7·26	9·19	12·49
	Drag D/q	0·138	0·163	0·211
	C.P. per cent wing chord aft of wing leading edge	7·2	30·4	39·6
15-deg Cone	Lift-curve slope $\frac{\partial(L/q)}{\partial\alpha}$	7·33	9·25	12·16
	Drag D/q	0·209	0·233	0·268
	C.P. per cent wing chord aft of wing leading edge	77·2	88·3	77·9

10
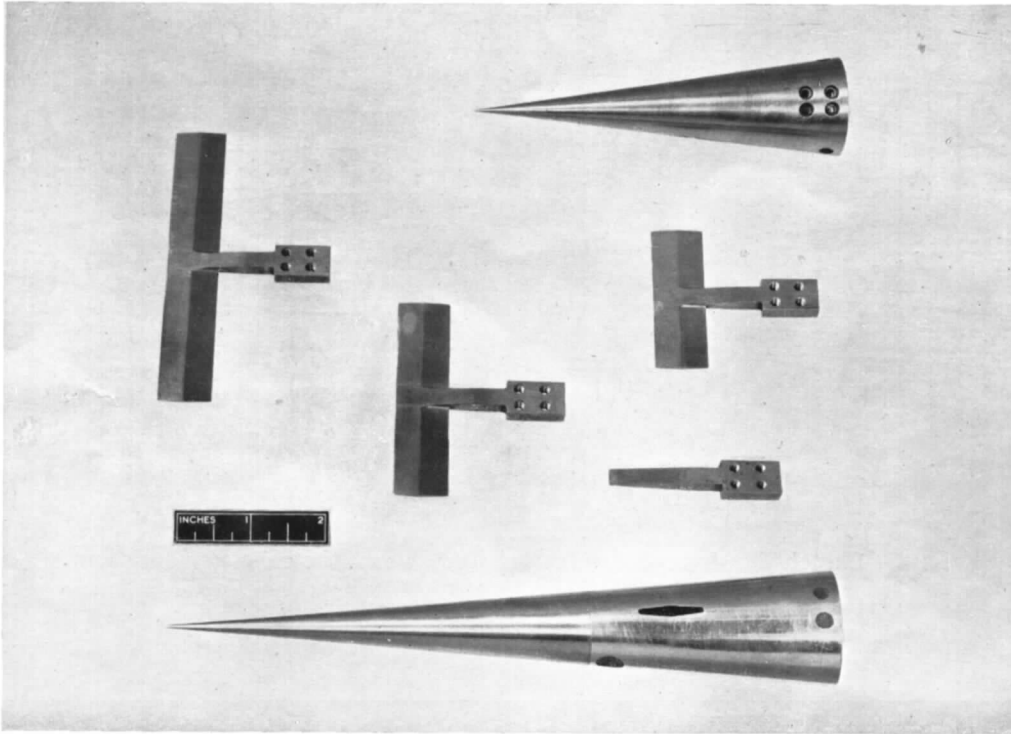
FIG. 1.   Cone and wing models.
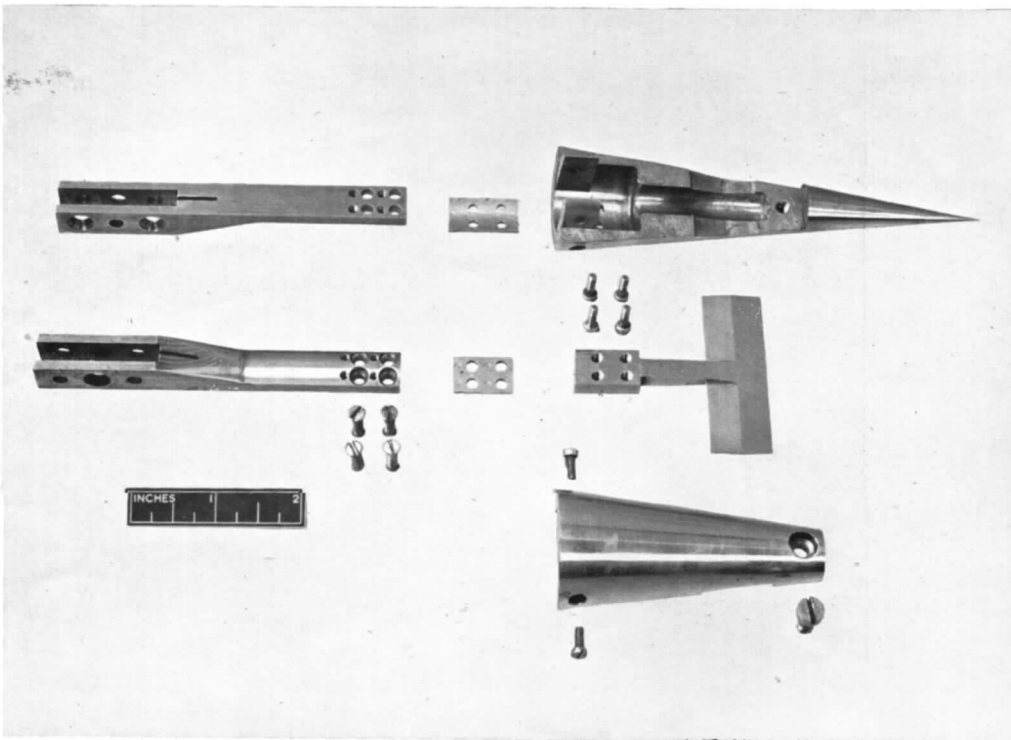
FIG. 2.   Components of 15-deg cone and wing assembly of aspect ratio 3.

11
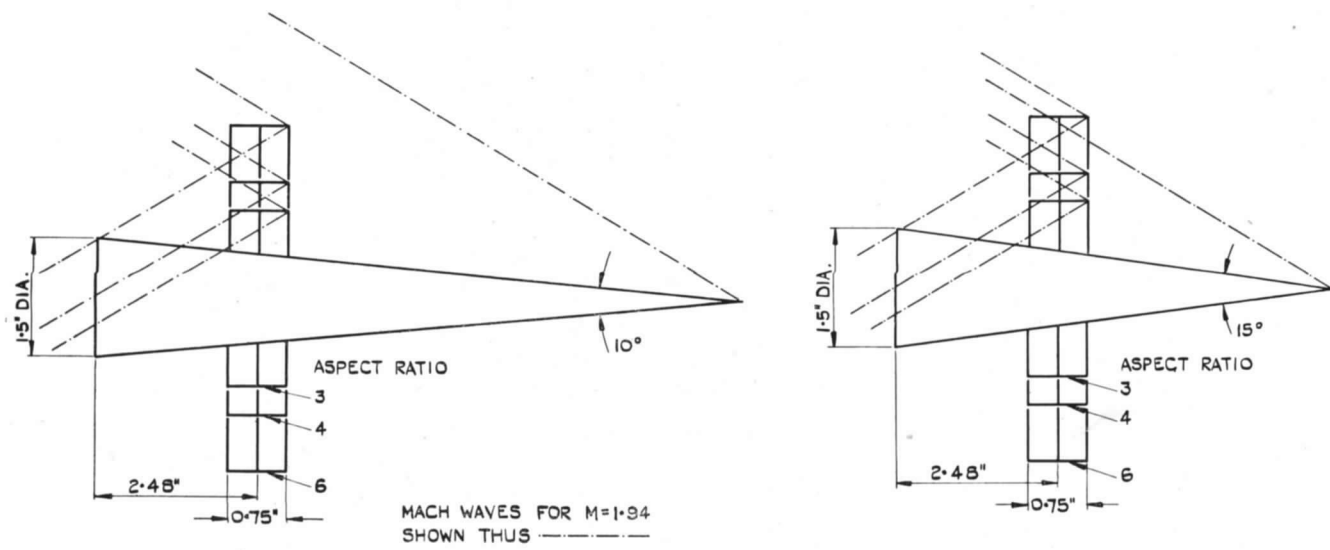
FIG. 3. Sketch showing Mach wave intersections on the cone configurations.
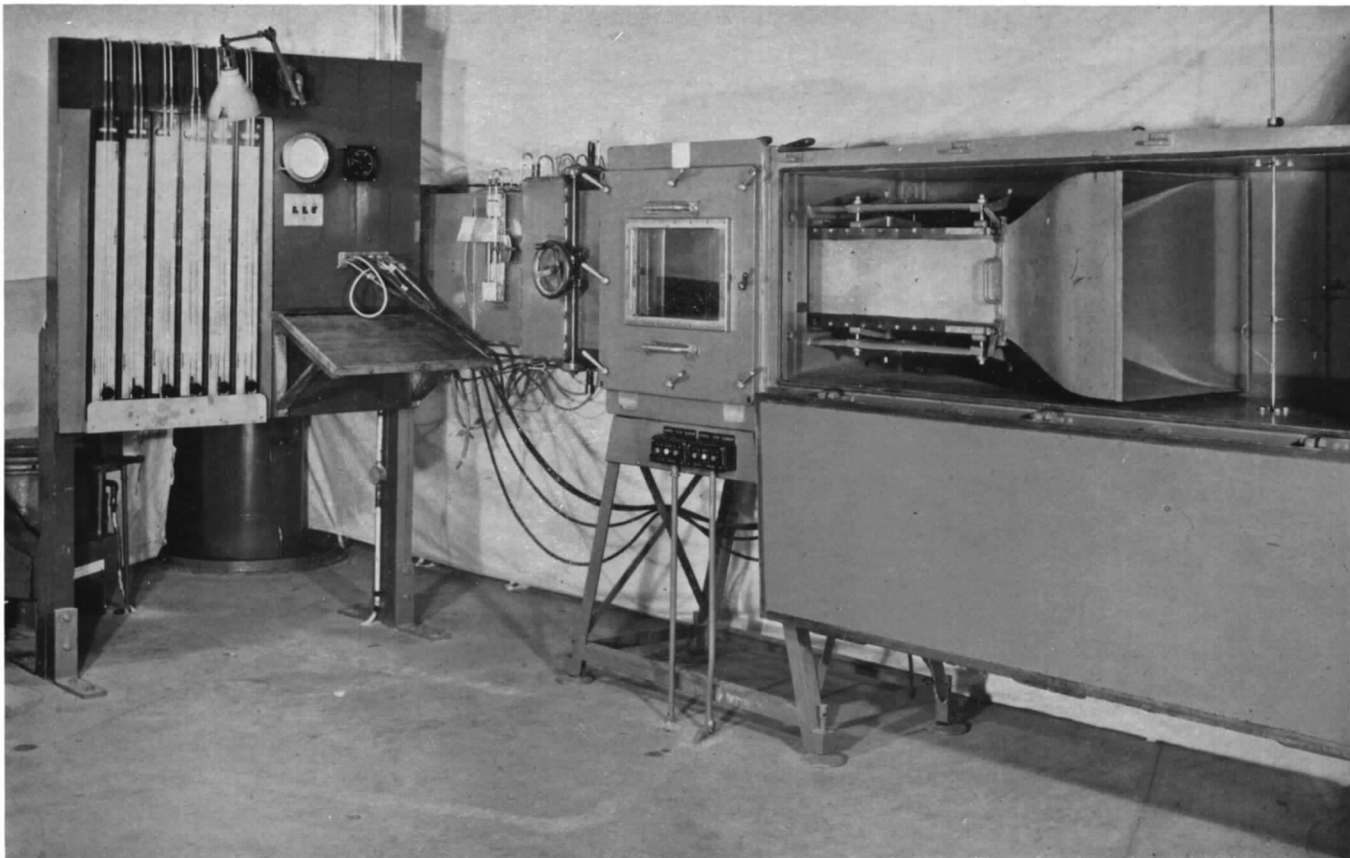
FIG. 4. General view of No. 8 Supersonic Wind Tunnel, showing contraction and nozzle box assembly (entry chamber open).

12
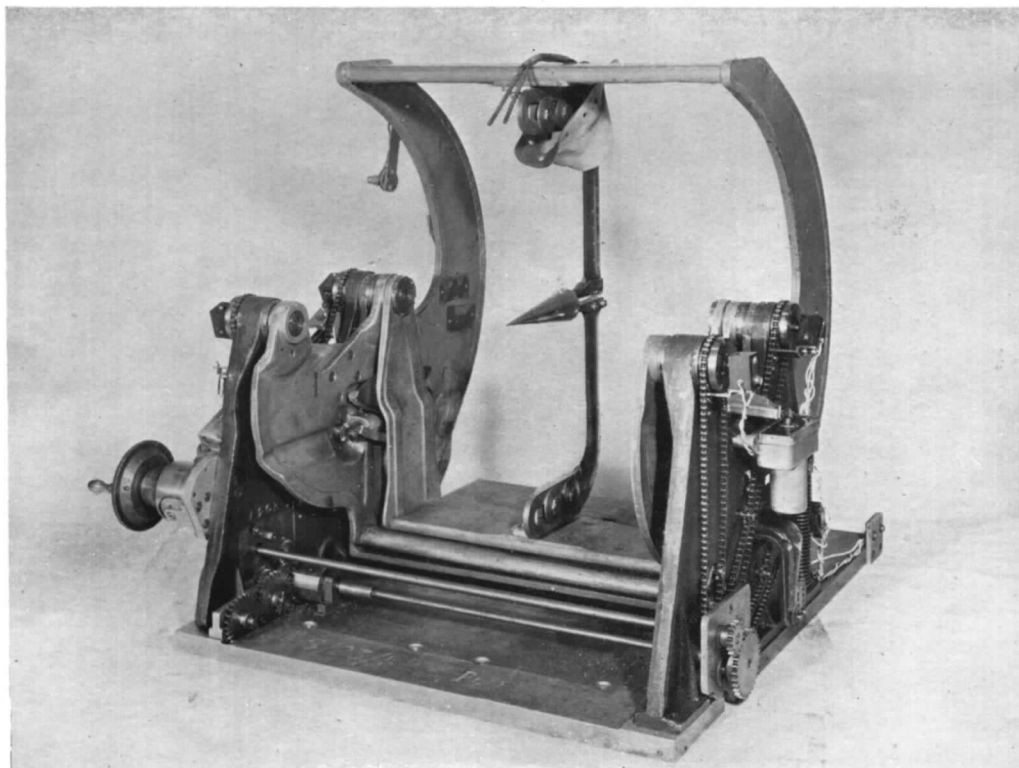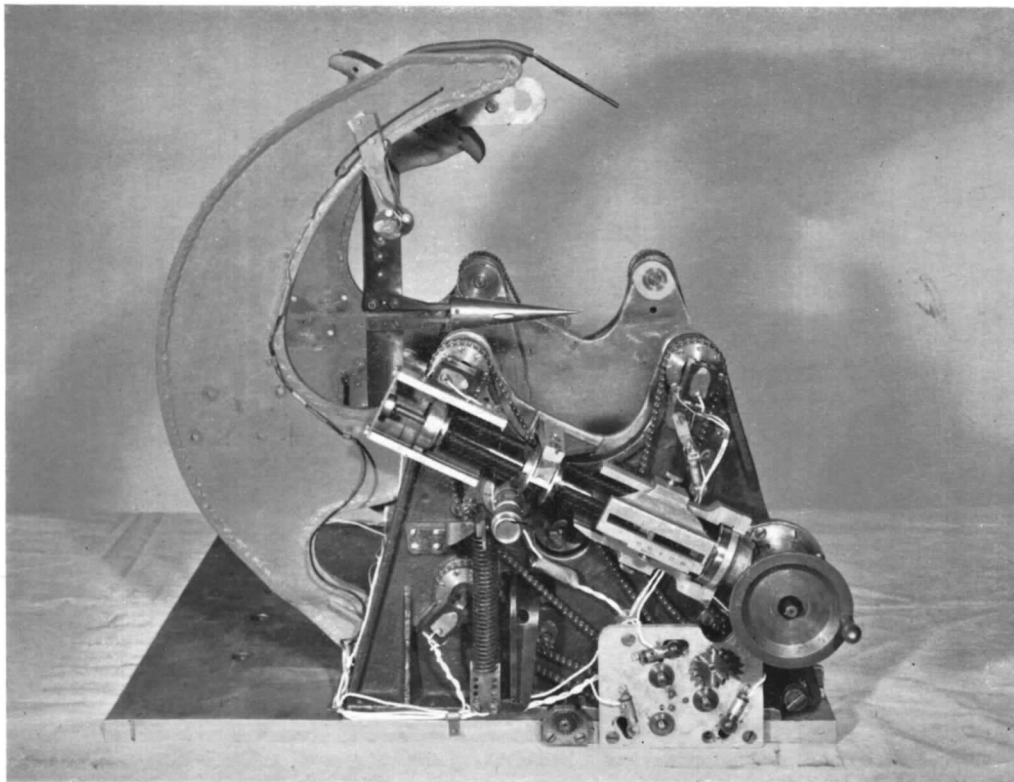
FIG. 5.   Three-component moment balance with all shielding removed.

13

14
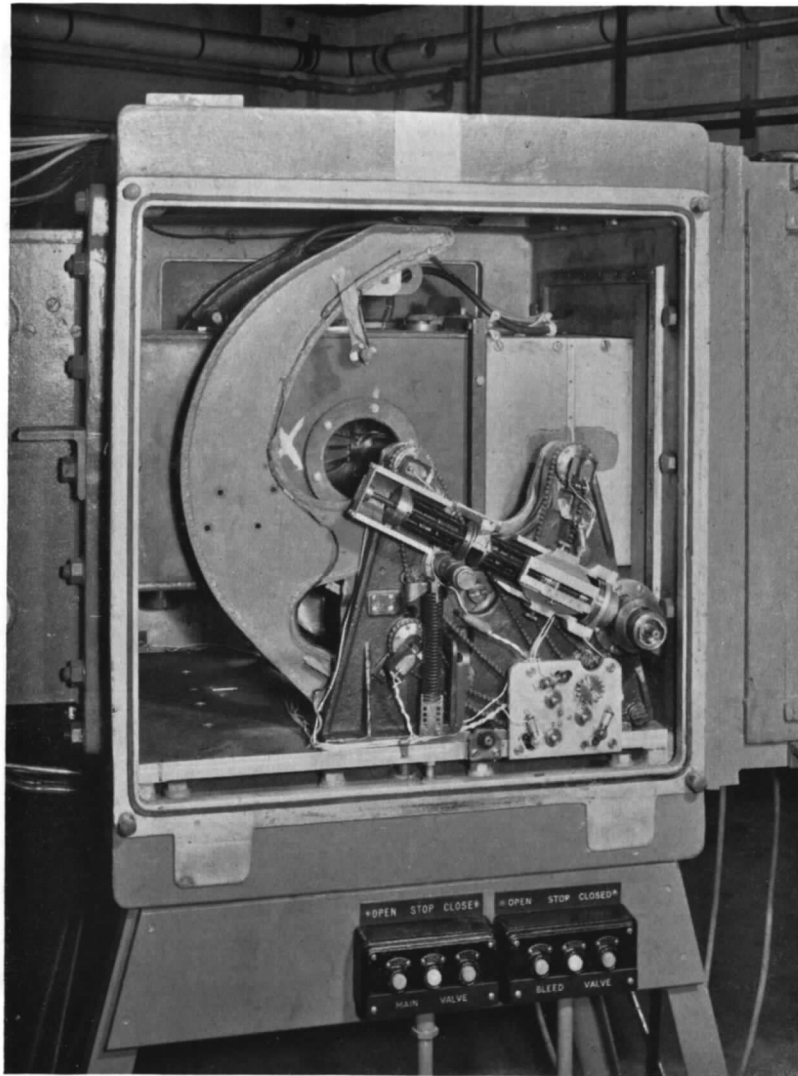
FIG. 6a.   Normal running.
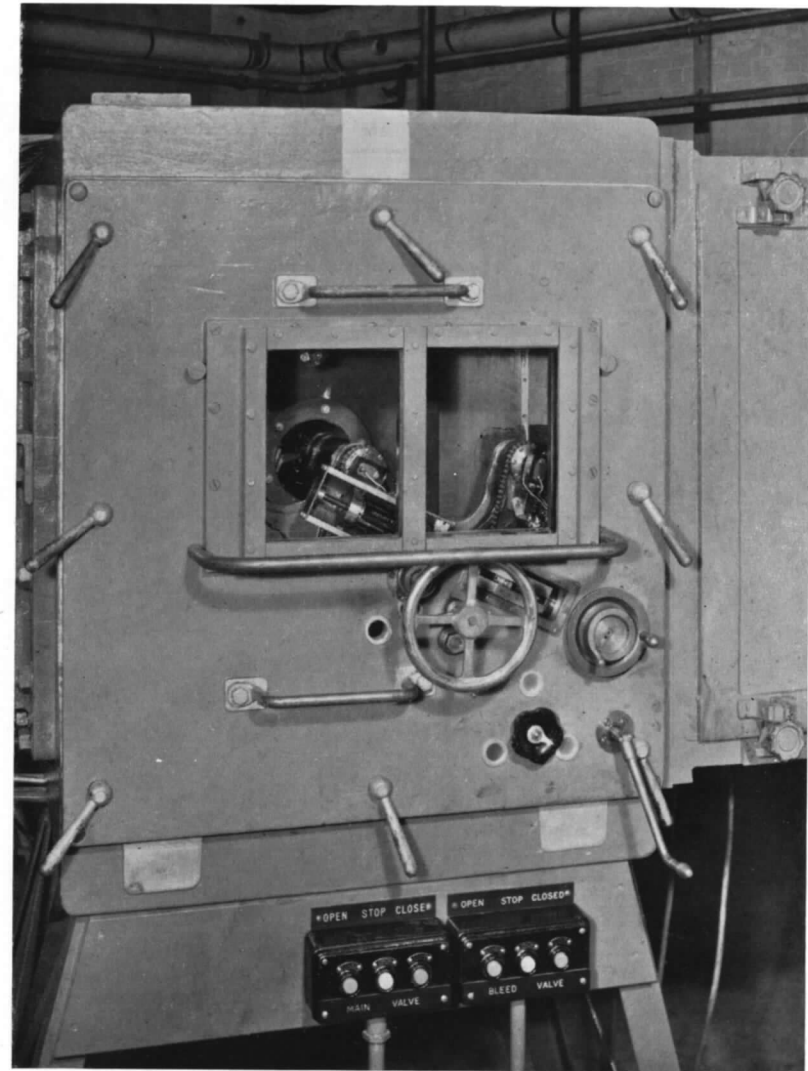
Fig. 6b.   Side door removed.

FIGS. 6a and 6b.   Balance chamber showing balance, internal duct and shielding.

FIG. 6c. Duct side plate removed.
Balance chamber showing balance, internal duct and shielding.

15
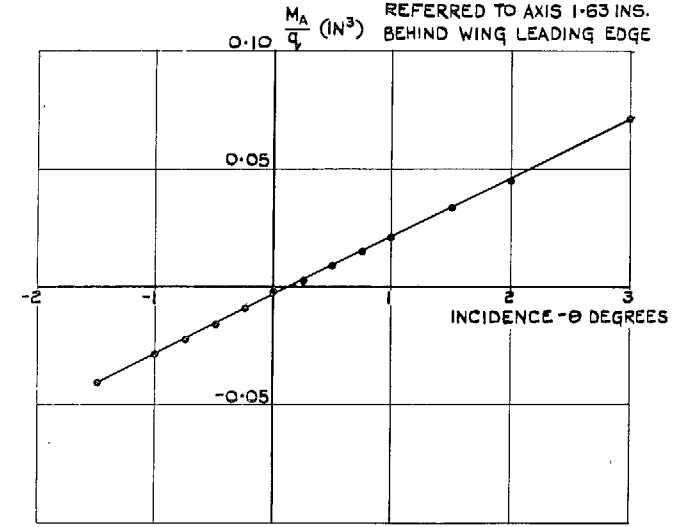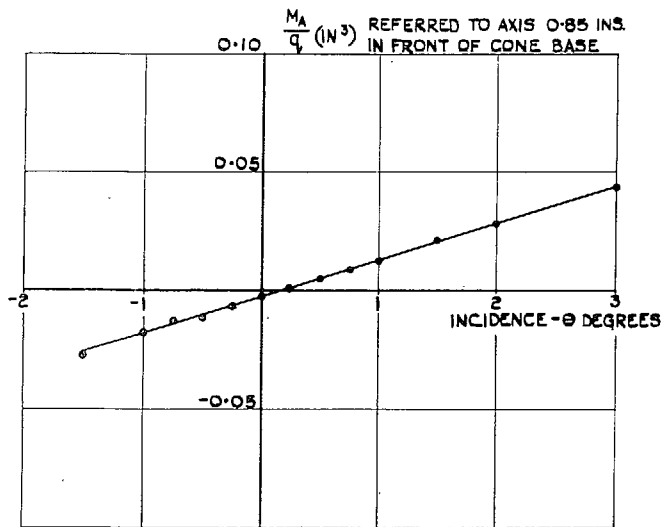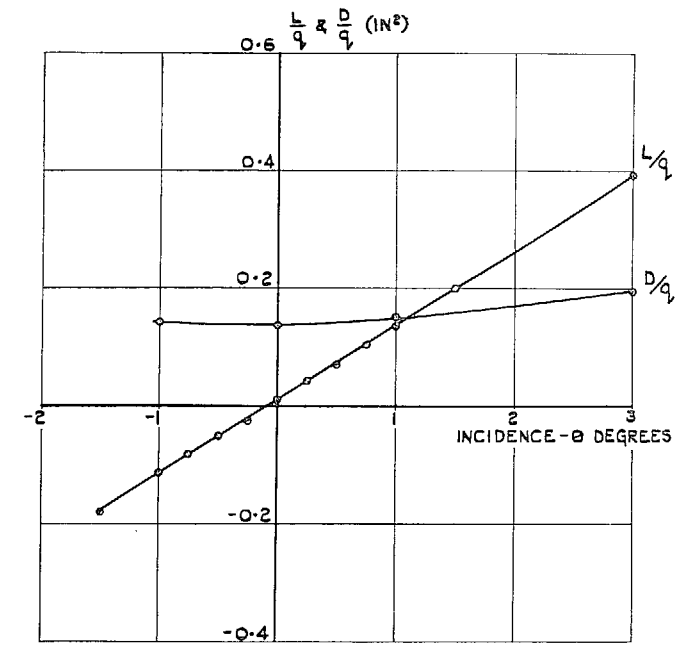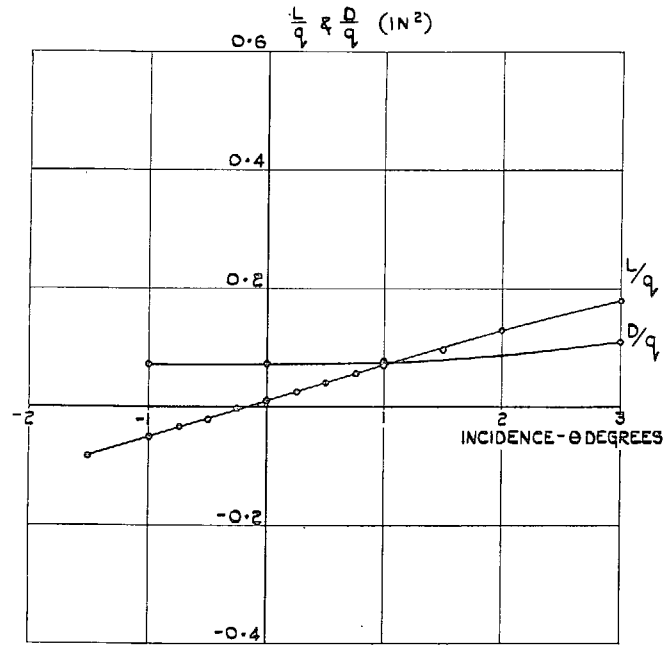
FIG. 7. Variation of lift, drag and moment with
incidence for 10-deg cone (C10).

FIG. 8. Variation of lift, drag and moment with
incidence for 10-deg cone with A=3 wing (C10W3).

16
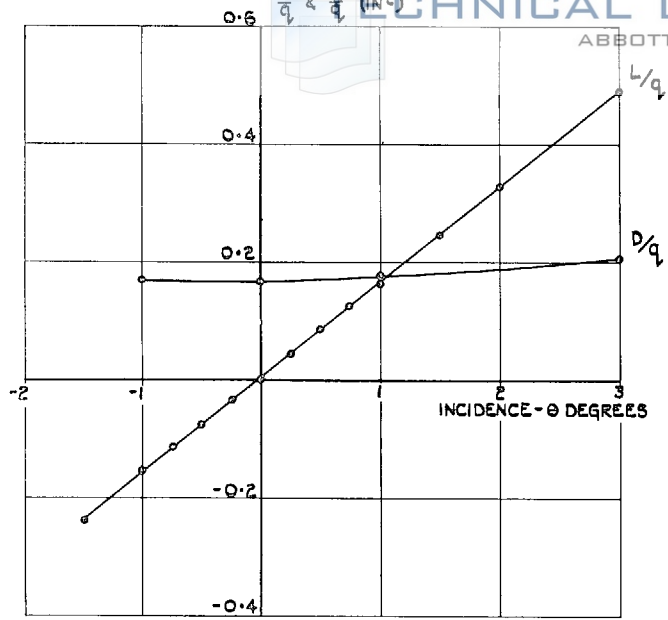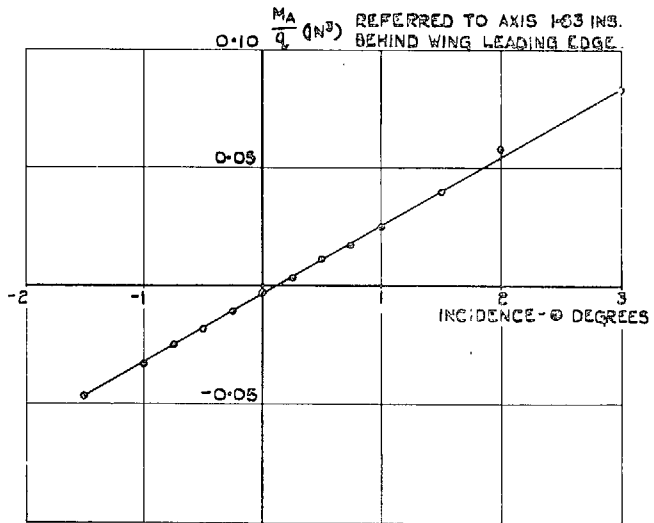
FIG. 9. Variation of lift, drag and moment with incidence for 10-deg cone with A=4 wing (C10W4).
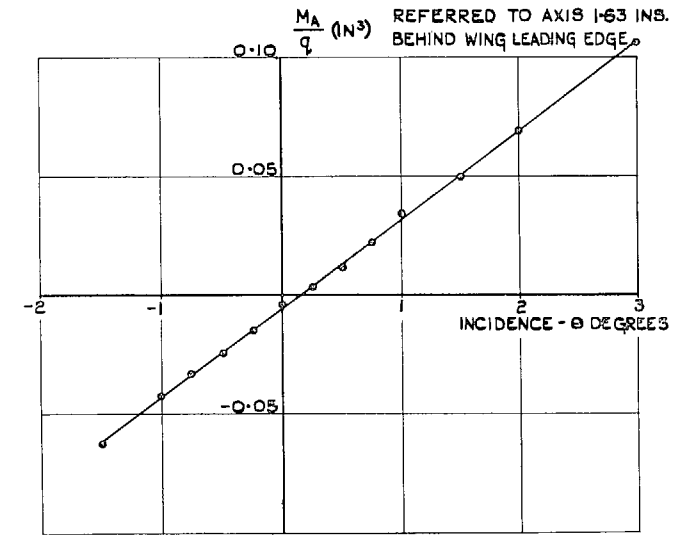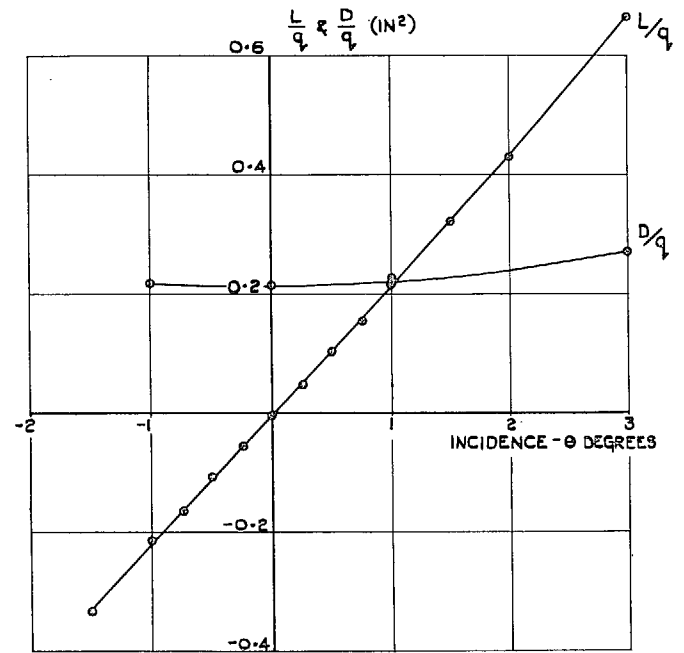
FIG. 10. Variation of lift, drag and moment with incidence for 10-deg cone with A=6 wing (C10W6).
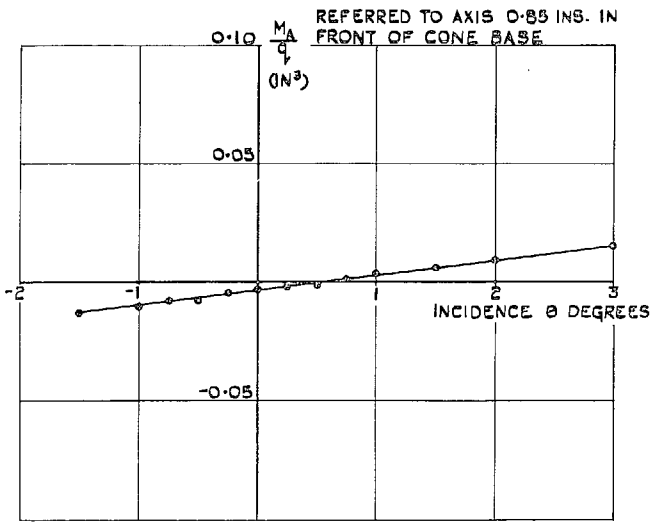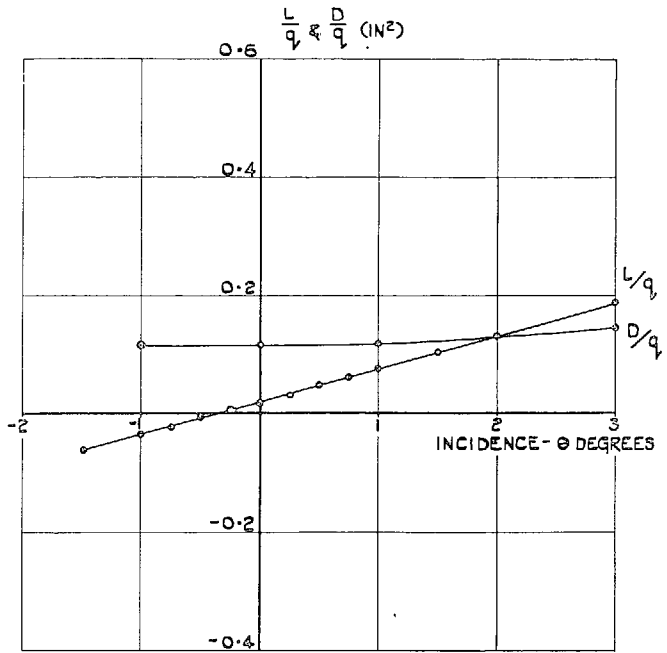
FIG. 11. Variation of lift, drag and moment with incidence for 15-deg cone (C15).
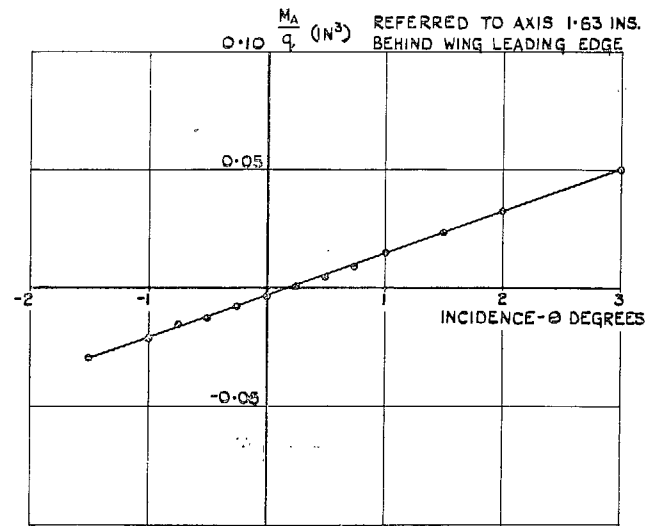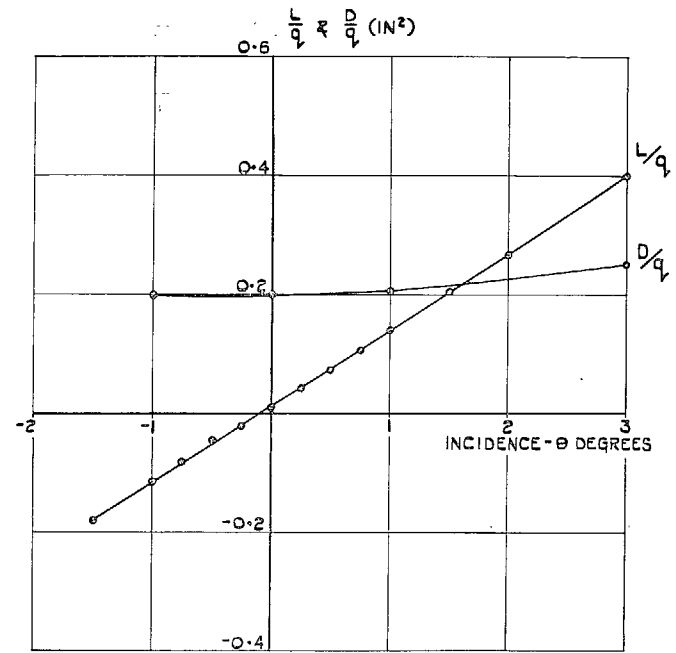
FIG. 12. Variation of lift, drag and moment with incidence for 15-deg cone with A=3 wing (C15W3).

19
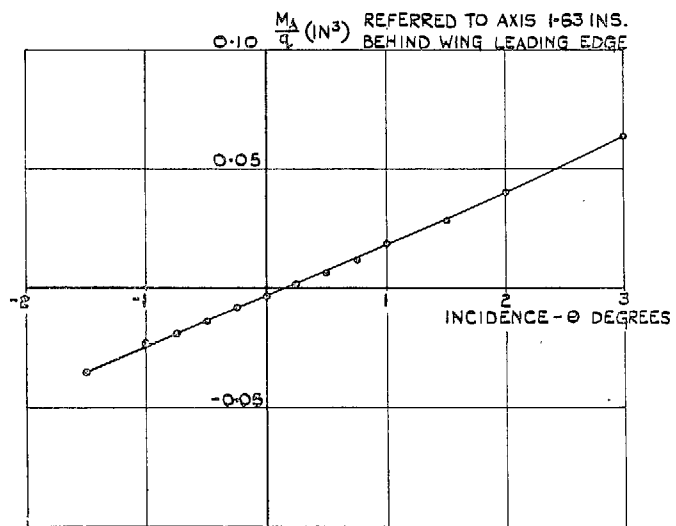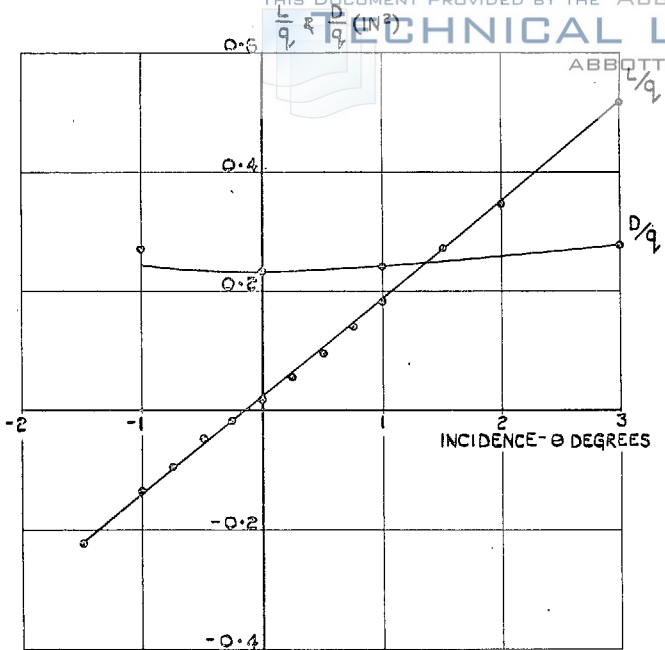
Fig. 13. Variation of lift, drag and moment with incidence for 15-deg cone with A=4 wing (C15W4).
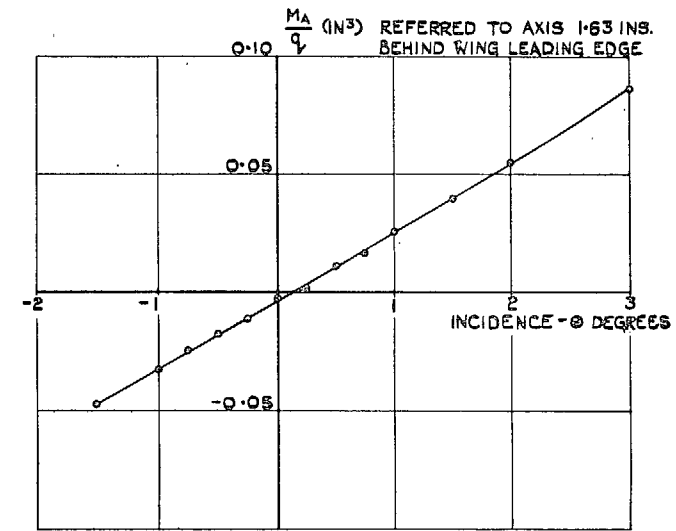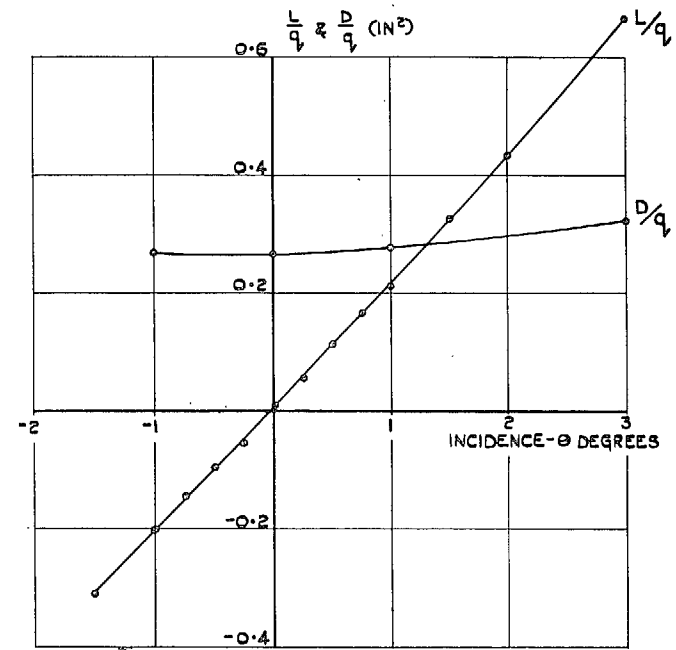
Fig. 14. Variation of lift, drag and moment with incidence for 15-deg cone with A=6 wing (C15W6).
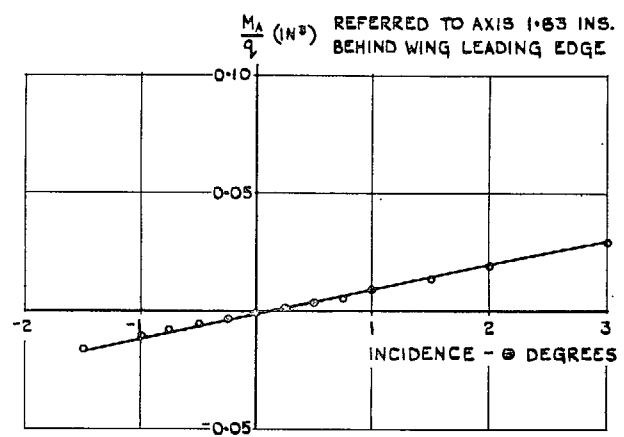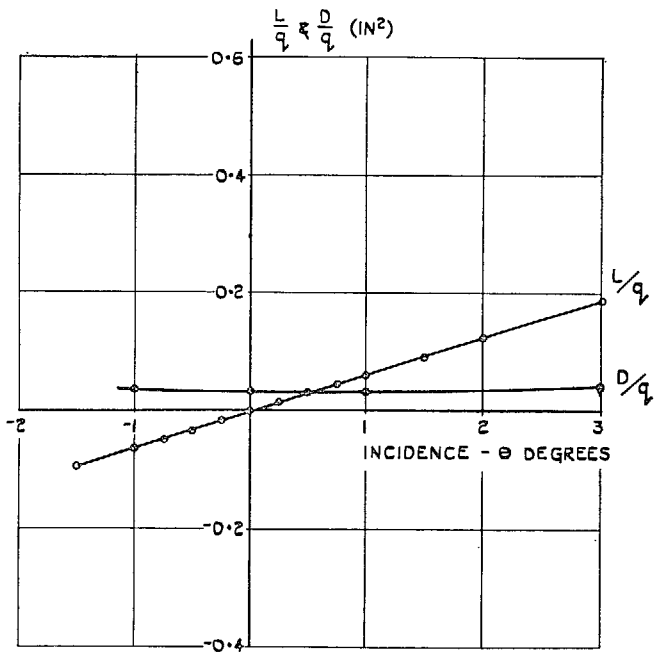
FIG. 15.   Variation of lift, drag and moment with incidence for $\frac{A=1}{A=3}$ 3 wing (W3).
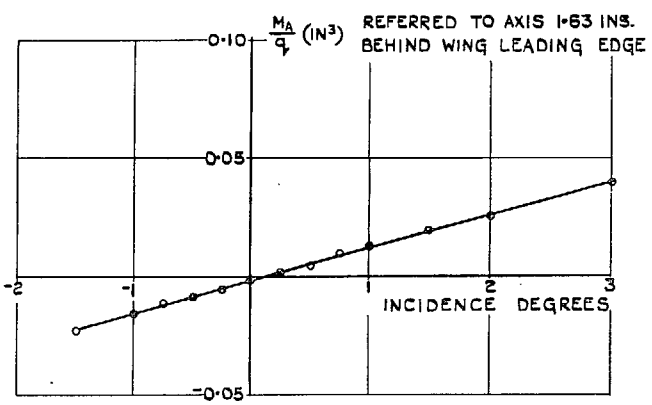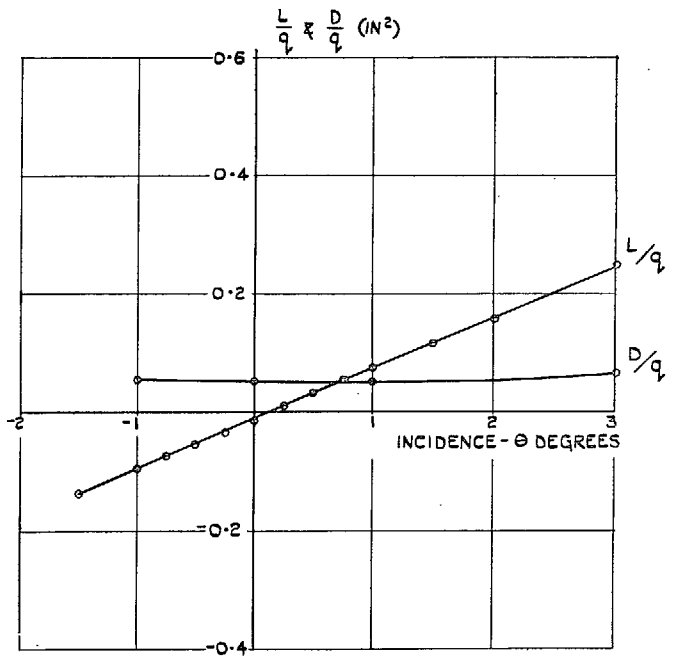
FIG. 16.   Variation of lift, drag and moment with incidence for $\frac{A=1}{A=4}$ 4 wing (W4).
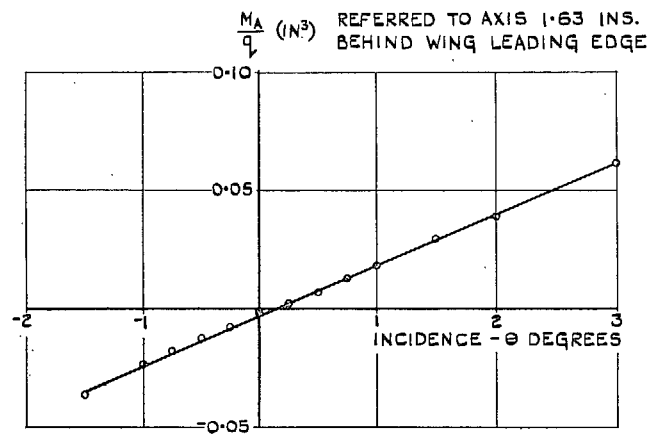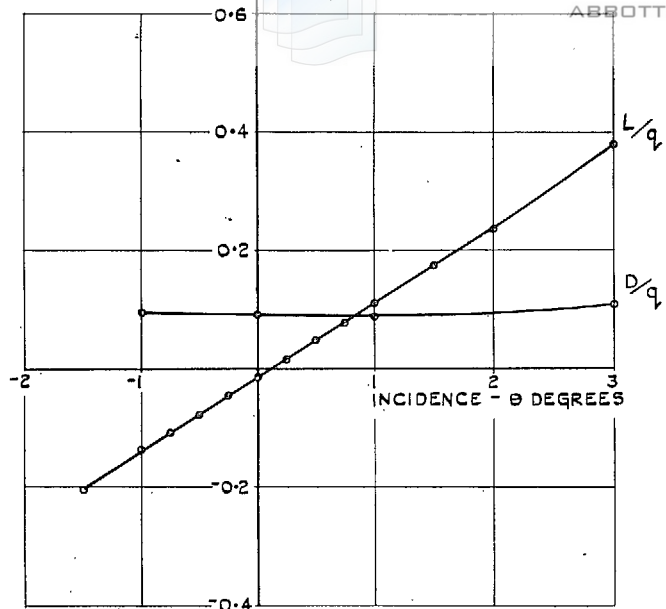
FIG. 17. Variation of lift drag and moment with incidence for $\begin{array}{c}A=1\\A=6\end{array}$ 6 wing (W6)
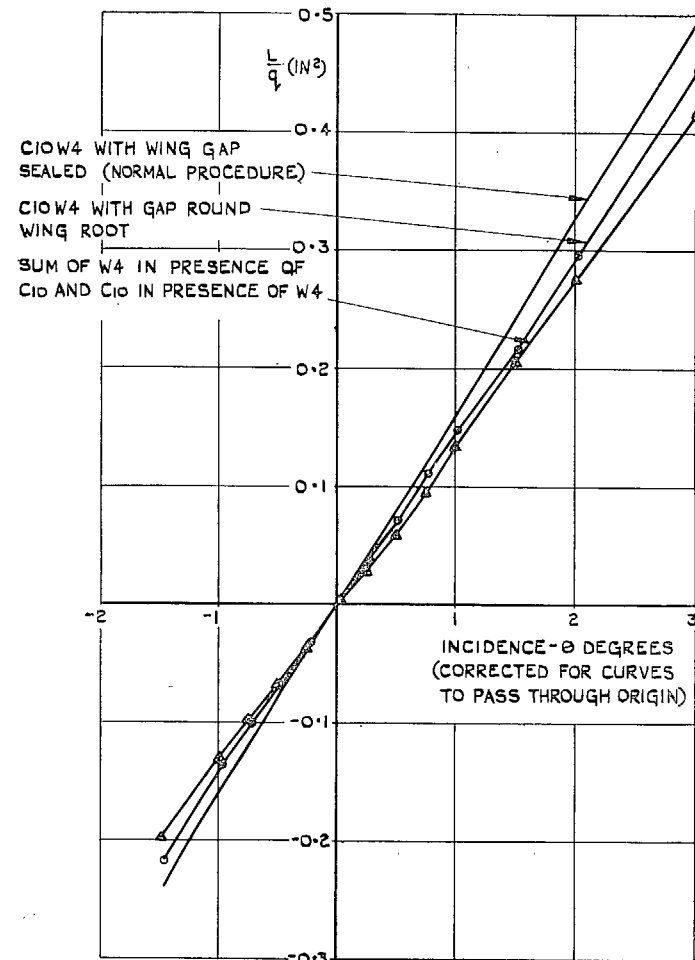
FIG. 18. Comparison of the lift of C10W4 with the lift of the combination with root clearance, and the sum of the individual components.
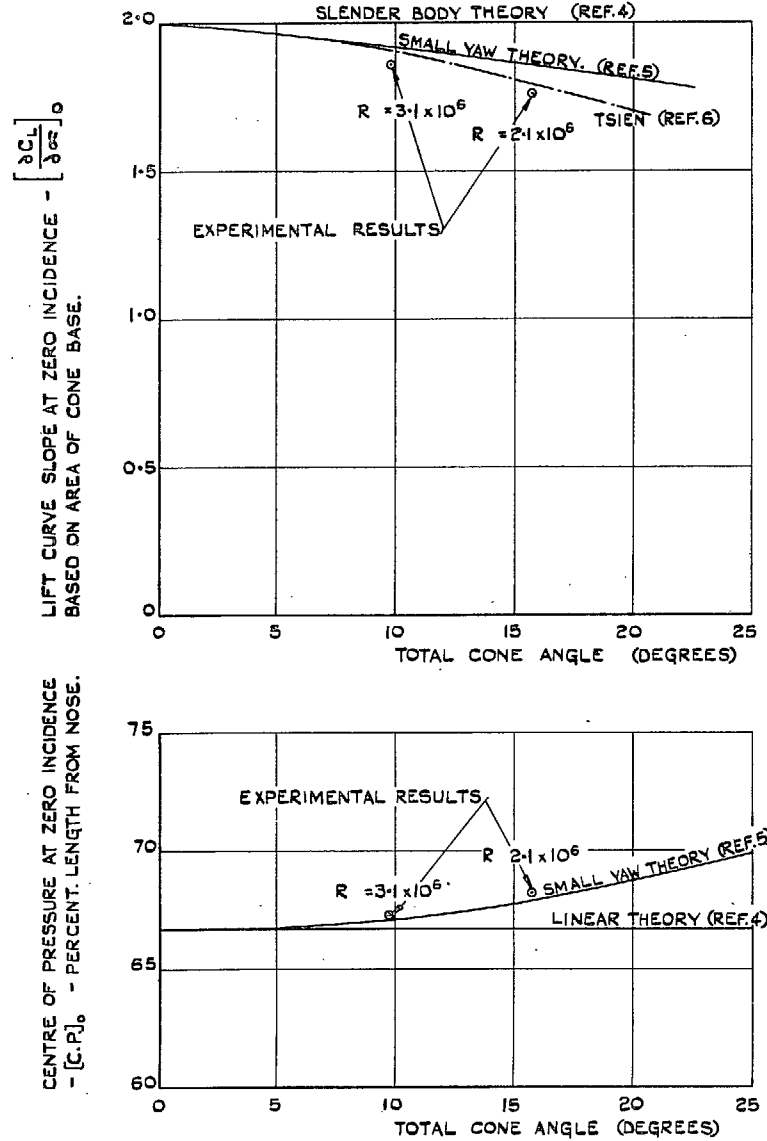
FIG. 19. Comparison of experimental and theoretical
$[\partial C_L/\partial\alpha]_0$ and $[c.p.]_0$ for cones at $M=1\cdot94$.
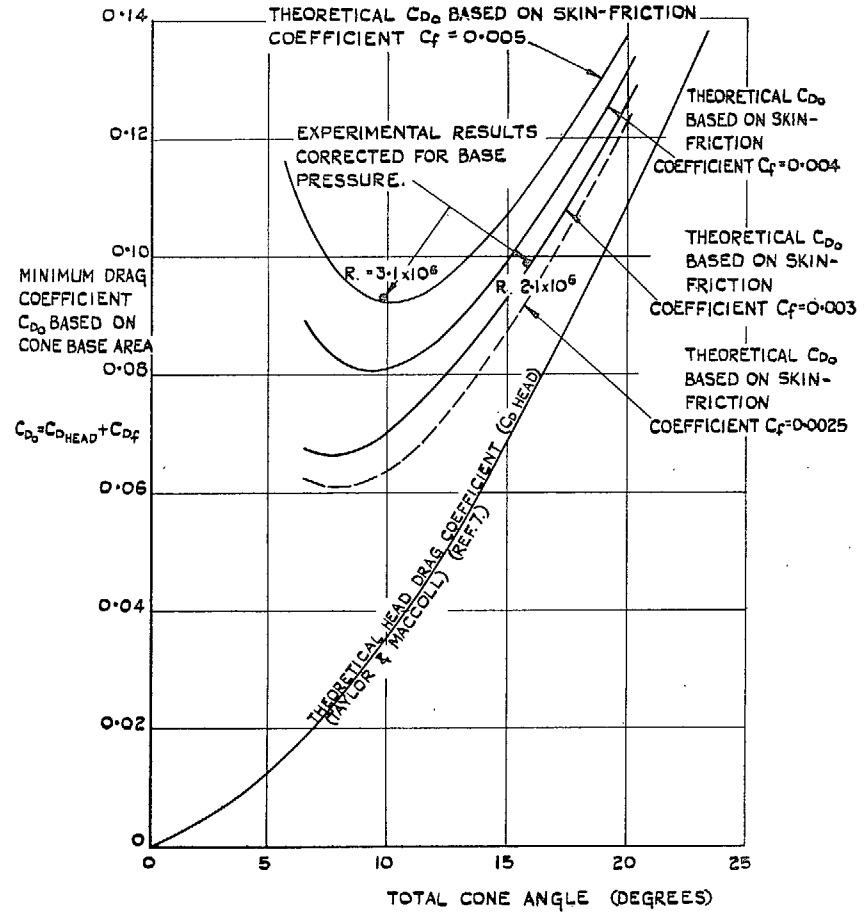
FIG. 20. Comparison of experimental and theoretical
$C_{D\,0}$ for cones at $M=1\cdot94$.

22
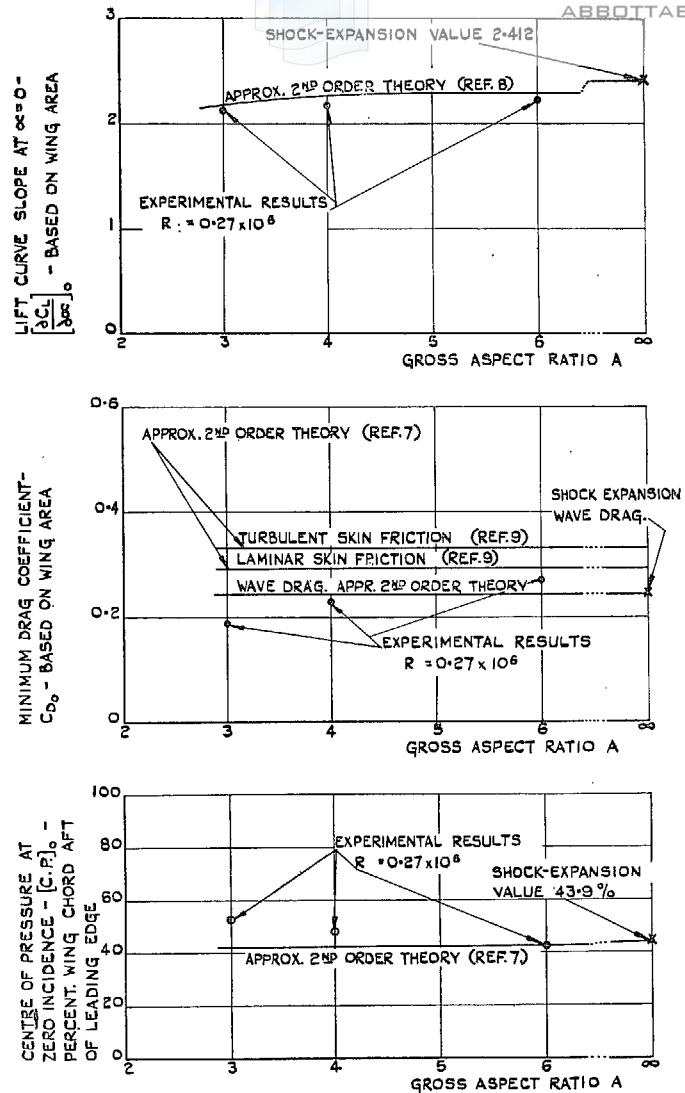
FIG. 21.   Comparison of Experimental and theoretical $[\partial C_L/\partial \alpha]_0$, C_{D0} and $[c.p.]_0$ for wings at $M = 1 \cdot 94$.
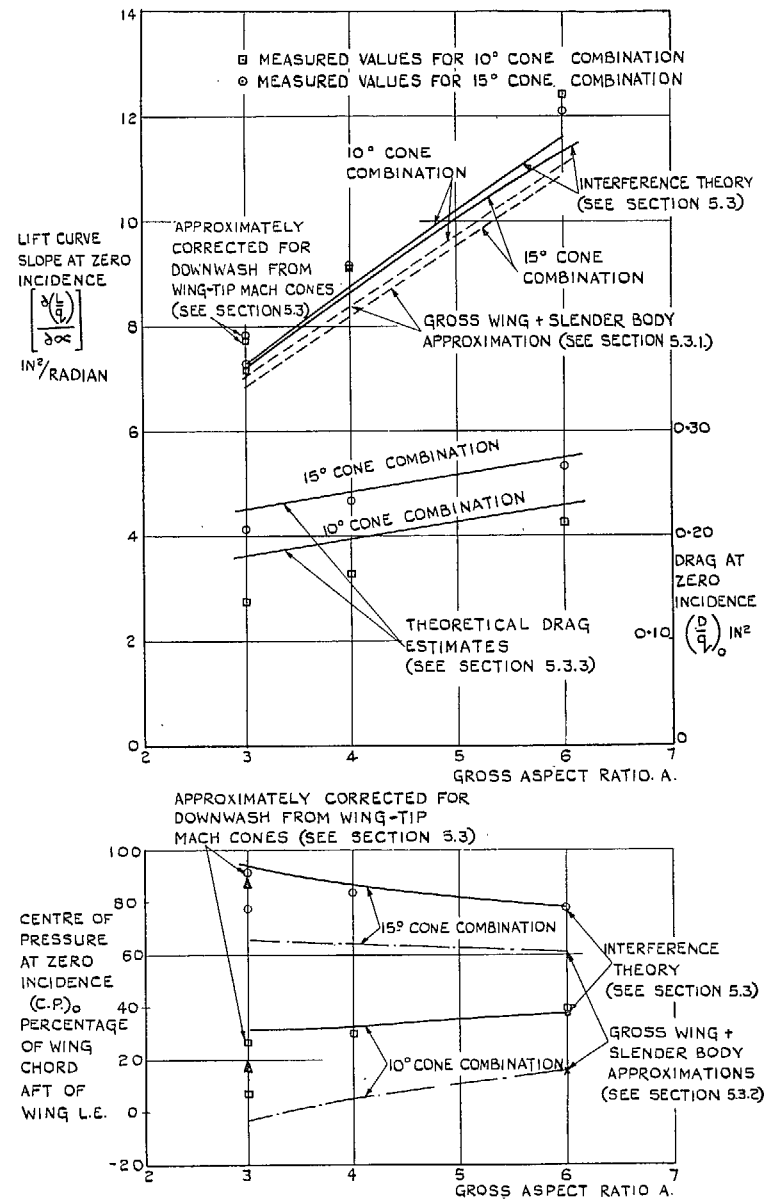
FIG. 22.   Comparison of experimental and theoretical $[\partial (L/q)/\partial \alpha]_0$, $[D/q]_0$ and $[c.p.]_0$ for wing-cone combinations at $M = 1 \cdot 94$.

23
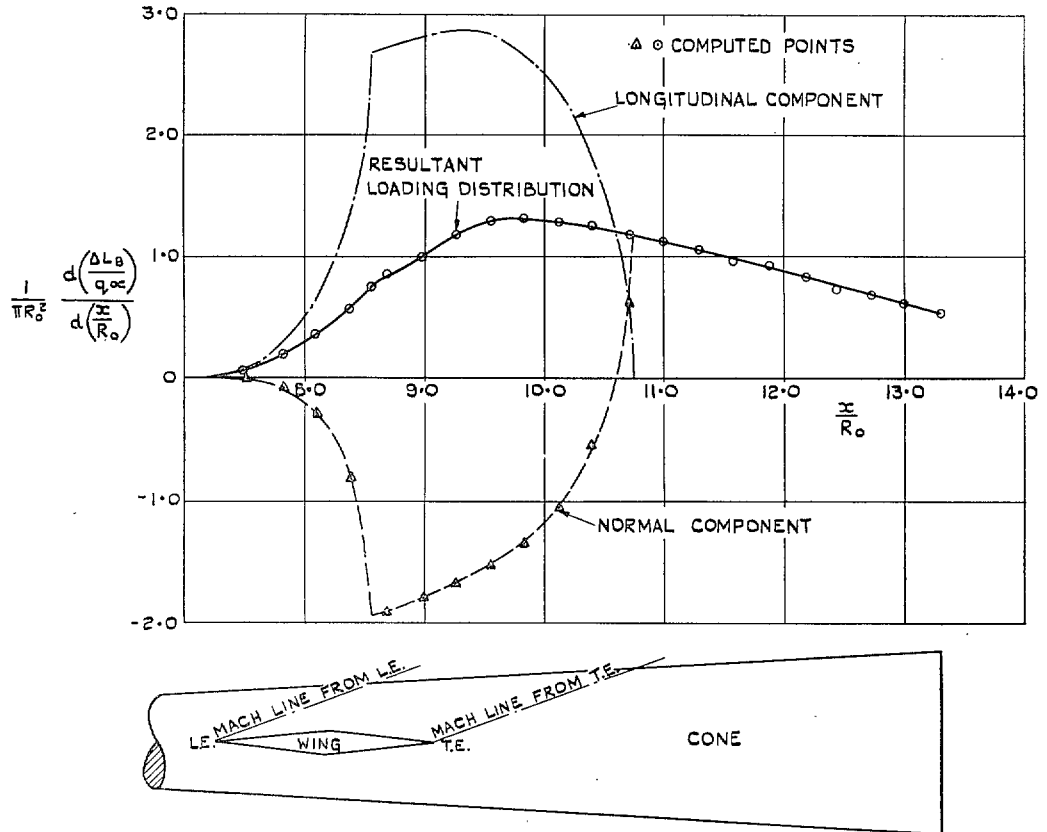
FIG. 23.   Increment in loading distribution along the 15-deg cone due to presence of wing at $M = 1 \cdot 5$.
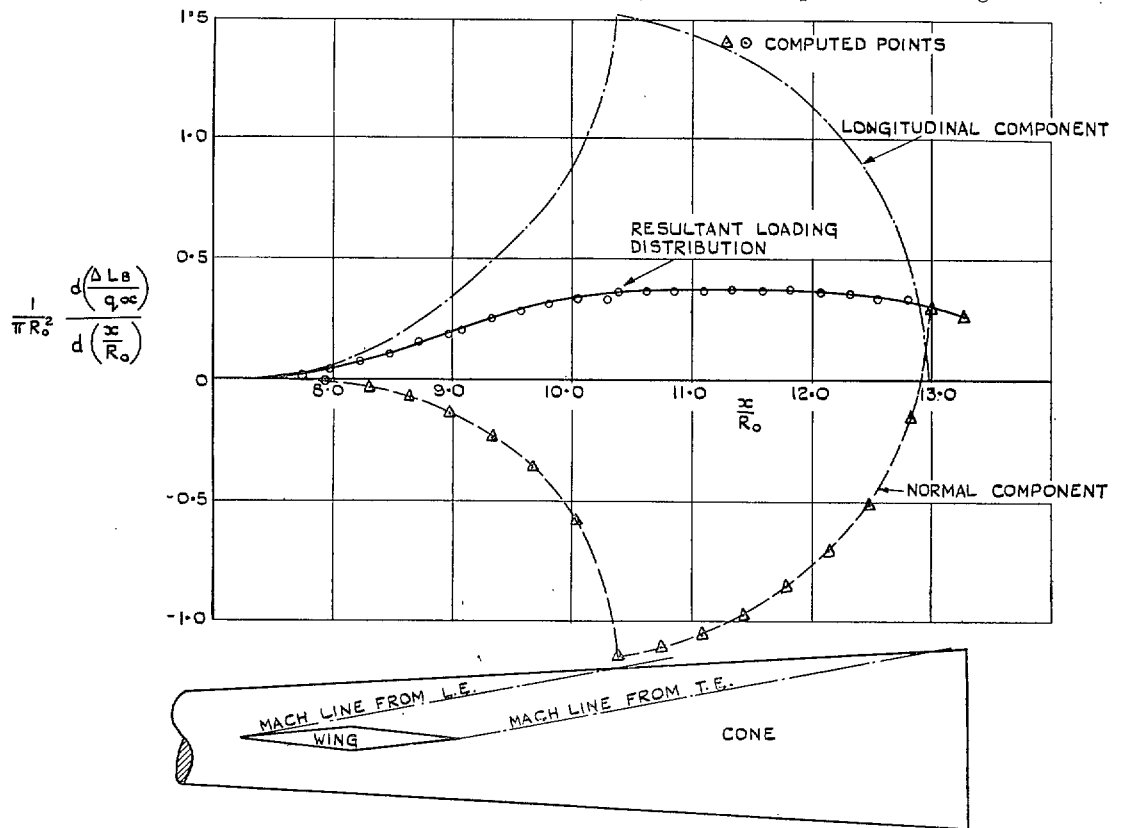
FIG. 24.   Increment in loading distribution along the 15-deg cone due to presence of wing at $M = 2 \cdot 4$.
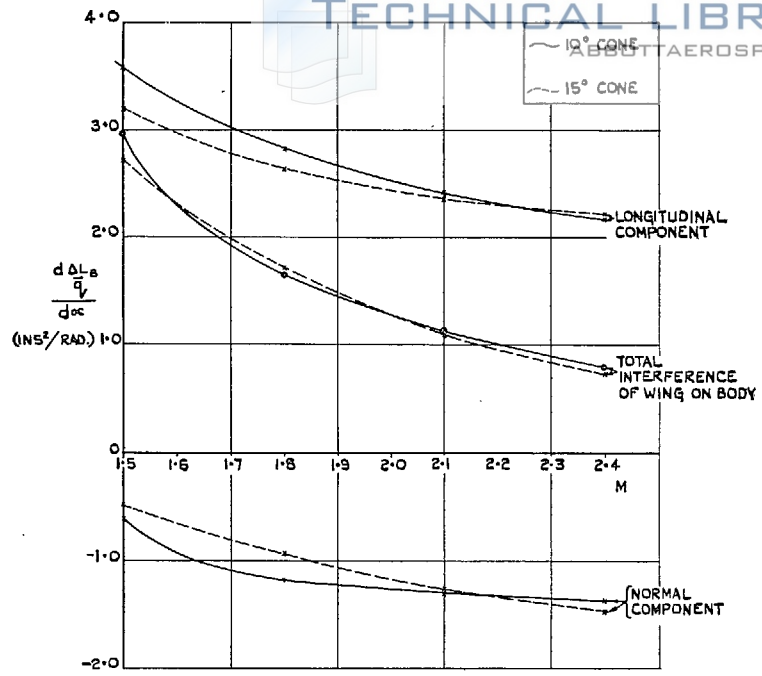
24
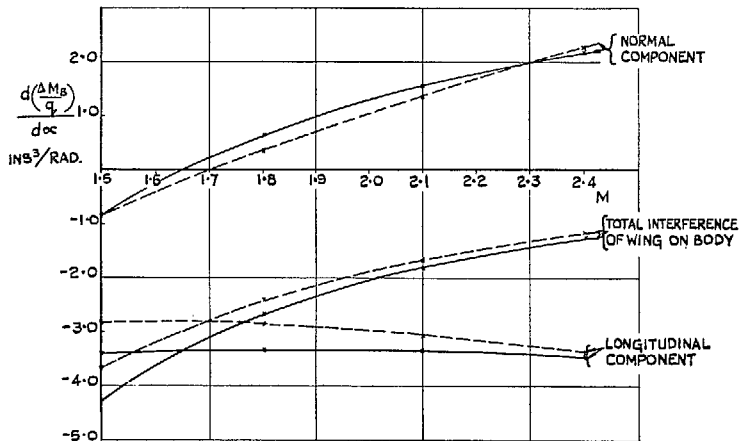
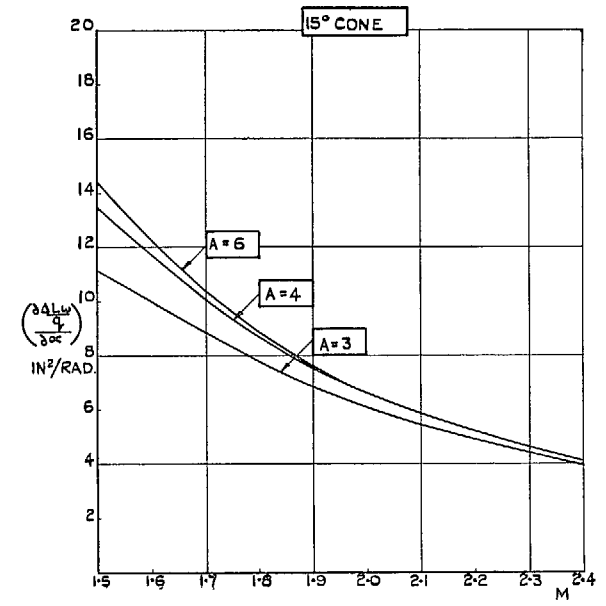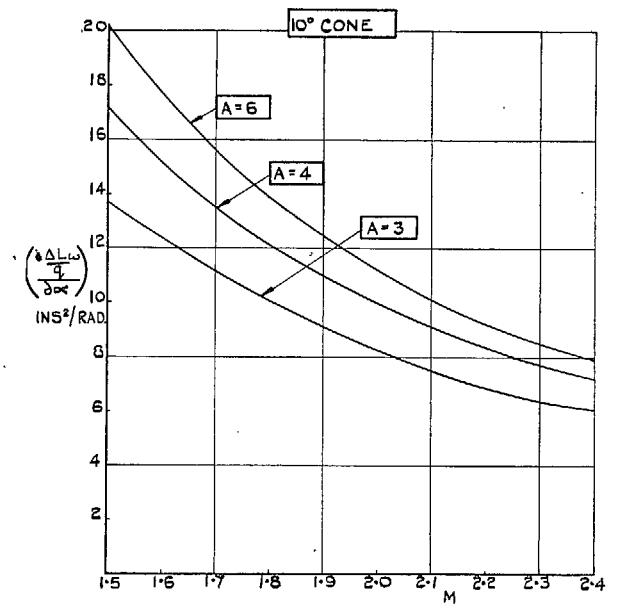FIG. 25.   Interference of wing on body (by method of Ref. 10).

FIG. 26.   Interference of body on wing (for 10-deg and 15-deg cones with rectangular wings of aspect ratios of 3, 4 and 6).

Publications of the
Aeronautical Research Council

ANNUAL TECHNICAL REPORTS OF THE AERONAUTICAL RESEARCH COUNCIL (BOUND VOLUMES)

1939 Vol. I. Aerodynamics General, Performance, Airscrews, Engines. 50s. (51s. 9d.)
　　 Vol. II. Stability and Control, Flutter and Vibration, Instruments, Structures, Seaplanes, etc. 63s. (64s. 9d.)

1940 Aero and Hydrodynamics, Aerofoils, Airscrews, Engines, Flutter, Icing, Stability and Control, Structures, and a miscellaneous section. 50s. (51s. 9d.)

1941 Aero and Hydrodynamics, Aerofoils, Airscrews, Engines, Flutter, Stability and Control Structures. 63s. (64s. 9d.)

1942 Vol. I. Aero and Hydrodynamics, Aerofoils, Airscrews, Engines. 75s. (76s. 9d.)
　　 Vol. II. Noise, Parachutes, Stability and Control, Structures, Vibration, Wind Tunnels. 47s. 6d. (49s. 3d.)

1943 Vol. I. Aerodynamics, Aerofoils, Airscrews. 80s. (81s. 9d.)
　　 Vol. II. Engines, Flutter, Materials, Parachutes, Performance, Stability and Control, Structures. 90s. (92s. 6d.)

1944 Vol. I. Aero and Hydrodynamics, Aerofoils, Aircraft, Airscrews, Controls. 84s. (86s 3d.)
　　 Vol. II. Flutter and Vibration, Materials, Miscellaneous, Navigation, Parachutes, Performance, Plates and Panels, Stability, Structures, Test Equipment, Wind Tunnels. 84s. (86s. 3d.)

1945 Vol. I. Aero and Hydrodynamics, Aerofoils. 130s. (132s. 6d.)
　　 Vol. II. Aircraft, Airscrews, Controls. 130s. (132s. 6d.)
　　 Vol. III. Flutter and Vibration, Instruments, Miscellaneous, Parachutes, Plates and Panels, Propulsion. 130s. (132s. 3d.)
　　 Vol. IV. Stability, Structures, Wind Tunnels, Wind Tunnel Technique. 130s. (132s. 3d.)

Annual Reports of the Aeronautical Research Council—

1937 2s. (2s. 2d.)　　　1938 1s. 6d. (1s. 8d.)　　　1939-48 3s. (3s. 3d.)

Index to all Reports and Memoranda published in the Annual Technical Reports, and separately—

April, 1950　　　　　R. & M. 2600.　　　2s. 6d. (2s. 8d.)

Author Index to all Reports and Memoranda of the Aeronautical Research Council—

1909–January, 1954.　　　R. & M. No. 2570　　15s. (15s. 6d.)

Indexes to the Technical Reports of the Aeronautical Research Council—

December 1, 1936 — June 30, 1939.　R. & M. No. 1850.　1s. 3d. (1s. 5d.)
July 1, 1939 — June 30, 1945.　　　R. & M. No. 1950.　1s. (1s. 2d.)
July 1, 1945 — June 30, 1946　　　R. & M. No. 2050.　1s. (1s. 2d.)
July 1, 1946 — December 31, 1946.　R. & M. No. 2150.　1s. 3d. (1s. 5d.)
January 1, 1947 — June 30, 1947.　　R. & M. No. 2250.　1s. 3d. (1s. 5d.)

Published Reports and Memoranda of the Aeronautical Research Council—

Between Nos. 2251–2349　　　R. & M. No. 2350.　1s. 9d. (1s. 11d.)
Between Nos. 2351–2449　　　R. & M. No. 2450.　2s. (2s. 2d.)
Between Nos. 2451–2549　　　R. & M. No. 2550.　2s. 6d. (2s. 8d.)
Between Nos. 2551–2649　　　R. & M. No. 2650.　2s. 6d. (2s. 8d.)

Prices in brackets include postage

HER MAJESTY'S STATIONERY OFFICE